DNA methylation epigenetically regulates gene expression in *Burkholderia cenocepacia*

Ian Vandenbussche[a], Andrea Sass[a], Marta Pinto-Carbó[b], Olga Mannweiler[b], Leo Eberl[b], Tom Coenye[a]#

[a] Laboratory of Pharmaceutical Microbiology, Ghent University, Ghent, Belgium

[b] Department of Plant and Microbial Microbiology, University of Zurich, Zurich, Switzerland

Running Head: Methylases regulate gene expression in *B. cenocepacia*

#Address correspondence to Tom Coenye, tom.coenye@UGent.be

Word Count Abstract: 232

Word Count Text: 4997

Abstract

Respiratory tract infections by the opportunistic pathogen *Burkholderia cenocepacia* often lead to severe lung damage in cystic fibrosis (CF) patients. New insights in how to tackle these infections might emerge from the field of epigenetics, as DNA methylation has shown to be an important regulator of gene expression. The present study focused on two DNA methyltransferases (MTases) in *B. cenocepacia* strains J2315 and K56-2, and their role in regulating gene expression. *In silico* predicted DNA MTase genes BCAL3494 and BCAM0992 were deleted in both strains, and the phenotypes of the resulting deletion mutants were studied: deletion mutant ΔBCAL3494 showed changes in biofilm structure and cell aggregation, ΔBCAM0992 was less motile. *B. cenocepacia* wild type cultures treated with sinefungin, a known DNA MTase inhibitor, exhibited the same phenotype as DNA MTase deletion mutants. Single-Molecule Real-Time sequencing was used to characterize the methylome of *B. cenocepacia*, including methylation at the origin of replication, and motifs CACAG and GTWWAC were identified as targets of BCAL3494 and BCAM0992, respectively. All genes with methylated motifs in their putative promoter region were identified and qPCR experiments showed an upregulation of several genes, including biofilm and motility related genes, in MTase deletion mutants with unmethylated motifs, explaining the observed phenotypes in these mutants. In summary, our data confirm that DNA methylation plays an important role in regulating the expression of *B. cenocepacia* genes involved in biofilm formation and motility.

Importance

CF patients diagnosed with *B. cenocepacia* infections often experience rapid deterioration of lung function, known as *cepacia syndrome*. *B. cenocepacia* has a large multi-replicon genome and a lot remains to be learned about regulation of gene expression in this organism. From studies in other (model) organisms, it is known that epigenetic changes through DNA methylation play an important role in this regulation. The identification of *B. cenocepacia* genes of which the expression is regulated by DNA methylation and identification of the regulatory systems involved in this methylation are likely to lead to new insights in how to tackle *B. cenocepacia* infections in CF patients.

Introduction

Burkholderia cenocepacia, a member of the *Burkholderia cepacia* complex (Bcc), is an aerobic Gram-negative bacterium that can be isolated from soil and water (1–3). *B. cenocepacia* is also known as an opportunistic pathogen in immunocompromised patients (4–6). Infection of the upper airways in cystic fibrosis (CF) patients often leads to severe illness, typically referred to as *cepacia syndrome* (1,7). CF patients diagnosed with *cepacia syndrome* experience a progressive decrease in lung function, often accompanied by bacteremia and sepsis. If left untreated, *cepacia syndrome* can lead to death within weeks (8,9). The genome of *B. cenocepacia* is complex (with usually three large replicons), with a high GC-content (67%) and large size, comprising approximately 8.06 Mb (10). The species has been classified into different phylogenetic clusters and subdivided into lineages, including the highly transmissible ET-12 lineage that harbors *B. cenocepacia* strains J2315 and K56-2 (11,12).

Epigenetics is the study of heritable changes in gene expression without changes in the actual genomic sequence. In bacterial genomes, epigenetic control is exerted by DNA methyltransferase enzymes (MTases) (13–15). DNA MTases originate from restriction-modification (RM) systems, early defense mechanisms in bacteria with an active interplay between endonucleases and DNA MTases, which cleave foreign DNA but protect the own genome. In addition, discovery of orphan DNA MTases, enzymes without a cognate endonuclease, shows that DNA MTases are not exclusively dependent on the presence of the restriction part to function as regulator of gene expression (16).

DNA MTases interact with specific DNA recognition sites and transfer a CH_3-group from a methyl donor, mostly S-adenosyl methionine, to a cytosine (C_5-methyl cytosine or N_4-methyl cytosine) or adenine (N_6-methyl adenine) base (17,18). As methylated bases change the binding affinity of DNA binding proteins, methylation at regulatory regions allows bacteria to regulate gene expression at the level of transcription (19,20). While both cytosine and adenine methylation occur in eukaryotic and prokaryotic cells, C_5-methyl cytosine is the archetypal eukaryotic base methylation signature (16,21). Conversely, in prokaryotes, N_6-methyl adenine is the most important base modification involved in gene expression regulation (22). In addition to this, studies with DNA MTases *Dam* (deoxyadenosine methyltransferase) and *Dcm* (DNA cytosine MTase) in *Escherichia coli* have demonstrated that, besides having a regulatory function, DNA MTases also take part in crucial cellular processes like DNA replication initiation or methyl-directed mismatch repair (21,23).

Detection of (genome-wide) DNA methylation patterns has been challenging in the past. The use of specific restriction enzymes with affinity for methylated sites, followed by a comparison of the resulting fragment lengths gave a good impression of methylation of the treated DNA at one particular area, but global methylation analysis was until recently difficult at best (21,24). The rise of Next-Generation Sequencing and Single-Molecule Real-Time (SMRT) technologies tremendously improved quality of methylome analyses, but it also made it much more accessible (25,26). SMRT Sequencing uses a sequencing-by-synthesis approach with fluorescently labeled nucleotides. Pulse width, the signal of nucleotide incorporation, and interpulse duration, the time between two incorporations, allow to discriminate between incorporated bases and their methylation status (27).

The purpose of the present study is to understand how DNA methylation regulates gene expression in *B. cenocepacia*. To this end, a genome-wide methylome analysis was carried out, and genes under DNA methylation regulation were identified. Interpretation of the working mechanisms of these regulatory systems, might lead to new insights in how to tackle *B. cenocepacia* infections in CF patients.

Results

Identification of *B. cenocepacia* DNA MTases

All predicted DNA MTase genes in the *B. cenocepacia* J2315 genome were identified using REBASE (Table S1). DNA MTase genes BCAL3494 and BCAM0992, widely distributed within the genus *Burkholderia*, were selected for further analysis. Gene BCAL3494, located on the first replicon of *B. cenocepacia*, is a type III

methyltransferase that is part of a RM-system, together with a restriction enzyme encoded by the neighbouring gene BCAL3493. Gene BCAM0992 is located on the second replicon and apparently does not have any adjacent genes coding for restriction enzymes. The gene is classified as coding for a type II methyltransferase, i.e. the restriction and modification enzymes act separately and are not dependent on each other (28). To investigate the influence of BCAL3494 and BCAM0992 on bacterial physiology, deletion mutants were constructed (Figure S1). For the other DNA MTase genes in *B. cenocepacia* J2315 identified with REBASE (Table S1), homologues in different *Burkholderia* strains could not be found; these genes were not further investigated in the present study.

Phenotype of mutant strains

BCAL3494 and BCAM0992 were deleted in two *B. cenocepacia* strains, J2315 and K56-2, and the phenotype of the deletion mutants was investigated in detail. No differences in growth between wild type and mutant strains were observed when cultured in phosphate buffered mineral medium (Figure S2). Microscopic analysis clearly showed a different, more clustered biofilm morphology for both BCAL3494 deletion mutants (ΔBCAL3494) compared to wild type strains, whereas the biofilm structure of the BCAM0992 deletion mutants (ΔBCAM0992) did not differ from wild type (Figure 1A). Cell aggregation in planktonic cultures was investigated using flow cytometry (Figure 1B). The degree of aggregation in the BCAL3494 mutant strains was significantly higher (p-value J2315: 0.049, p-value K56-2: 0.001) than in the corresponding wild type strains. Also, the ability to form a pellicle, a biofilm-like structure at the air-liquid interface, was investigated (Figure 1C). Pellicle formation was clearly

136 increased for both ΔBCAL3494 mutants compared to wild type strains and to
137 ΔBCAM0992 mutants. Complemented mutant strains *c*ΔBCAL3494 and *c*ΔBCAM0992
138 did not differ significantly from wild type in these experiments (Figure S3).

139 Motility of all strains was assessed using a swimming motility assay on 0.3 %
140 agar plates. After 24h (strain K56-2), and 32h (strain J2315), plates were photographed
141 and diameters measured (Figure 2). Diameters were significantly smaller for both
142 ΔBCAM0992 mutants compared to wild type (p-value J2315: 0.002, p-value K56-2 <
143 0.001). Both ΔBCAL3494 mutants, as well as the complemented mutants, were
144 identical to wild type in this regard. We also investigated swarming motility, but no
145 significant differences between the different strains were observed (Figure S4).

146 **Effect of the DNA MTase inhibitor sinefungin on methylation-dependent**
147 **phenotypes**

148 Sinefungin, a structural analog of S-adenosyl methionine and known for blocking
149 base methylation in other bacteria such as *Streptococcus pneumoniae* (29), was used
150 as DNA MTase inhibitor. The minimum inhibitory concentration (MIC) of sinefungin in
151 *B. cenocepacia* J2315 and K56-2 was determined and was found to be higher than 200
152 µg/mL. Both strains were exposed to sinefungin concentrations below the MIC of
153 sinefungin (50 µg/mL) to assure any effect observed was not due to growth inhibition by
154 sinefungin, and the effect on biofilm formation, pellicle formation, cell aggregation and
155 motility was quantified (Figure 3). Bacteria exposed to sinefungin produced more pellicle
156 mass, showed a higher degree of cell aggregation (p-value: 0.003), had a different
157 biofilm morphology, and were less motile (p-value: 0.004). These findings indicate that

chemically blocking DNA methylation or deleting genes responsible for DNA methylation lead to the same phenotypes in *B. cenocepacia* J2315 and K56-2.

Methylome analysis

Using SMRT sequencing (PacBio), the complete methylome of *B. cenocepacia* J2315 and K56-2 was identified. Only data for strain J2315 are reported in the following section, as data for strain K56-2 were highly comparable (Figures 4 and 5). Three distinct methylated motifs were identified in the wild type strain: CACAG, GTWWAC, and GCGGCCGC. The CACAG motif was methylated at the fourth position on the forward strand, whereas the GTWWAC motif was methylated at the fifth position on both the forward and reverse strand. Cytosine methylation of the GCGGCCGC motif occurred at the fifth position on both the forward and reverse strand. Although all CACAG and GTWWAC motifs were methylated in the wild type strains, methylation of the CACAG motif was absent in the ΔBCAL3494 deletion mutants, and likewise, no methylation of the GTWWAC motif was seen in the ΔBCAM0992 mutants (Table S2). This demonstrates that MTase BCAL3494 recognizes the CACAG motif, while MTase BCAM0992 recognizes the GTWWAC motif. In contrast, cytosine methylation of the GCGGCCGC motif was observed in wild type and in mutant strains, but the extent of methylation at this motif was highly variable in the four datasets. This suggests that this cytosine methylation occurs randomly, and that the GCGGCCGC motif might present a false positive result of motif analysis due to the high occurrence of short repeats of G and C in the GC-rich *B. cenocepacia* genome. In addition, almost no methylated GCGGCCGC motifs were found in regulatory regions, hinting at only a minor role for

cytosine methylation in regulation of gene expression. Therefore, cytosine methylation in *B. cenocepacia* was not further studied.

The location of every methylated CACAG and GTWWAC motif was mapped (Figures 4 and 5). A total of 6834 methylated CACAG motifs and 961 methylated GTWWAC motifs was found, of which the majority was present on the first replicon (CACAG: 45.6 %, GTWWAC: 49.9 %), followed by the second replicon (CACAG: 42.1 %, GTWWAC: 38.9 %), the third replicon (CACAG: 10.6 %, GTWWAC: 9.0 %), and the plasmid (CACAG: 1.7 %, GTWWAC: 2.2 %). Subsequently, all genes with methylated motifs in their promoter region, here defined as 60 bases upstream of the transcription start site, were identified. 91 promoter regions contained methylated CACAG motifs, and 80 promoter regions contained methylated GTWWAC motifs, with most of the motifs being present on the first replicon (Figures 4 and 5). Functional classes of genes found in the dataset of genes with methylated promoter include genes involved in intermediary metabolism, regulation, and transport (Tables S3 and S4).

Virtual Footprint was used to elucidate to which transcription factor (TF) binding sites the discovered methylation motifs CACAG and GTWWAC showed any similarity. Data output of the analysis is listed in Table S5. Sequences that contain methylation motif CACAG were similar to the binding site of *E. coli* K12 GlpR, while GTWWAC-containing sequences were similar to binding sites of several other *E. coli* K12 TFs, including ArcA, OxyR, Fis and Fur.

Expression of genes with a methylated promoter

The expression level of genes with methylated promoter regions was determined in wild type and mutant strains, using qPCR. Expression data of genes with methylated

promoter regions are listed in Tables 1 and 2. Volcano plots (Figure S5, fold changes plotted against corresponding p-values) show that most genes tested were upregulated in the mutants compared to the wild type strains. Six of these genes were significantly upregulated in mutants of both strain backgrounds: BCAL1515, BCAL2465, and BCAM0820 were upregulated in ΔBCAL3494, whereas genes BCAL0079, BCAL2415, and BCAM1362 were upregulated in ΔBCAM0992. Four additional genes were upregulated in K56-2 mutants only: BCAL0423, BCAM2738, and BCAS0223 were upregulated in ΔBCAL3494, BCAL1556 in ΔBCAM0992. Subsequently, the methylated promoter regions of these genes were analyzed in detail (Figure 6). In most cases, the methylated motif was in close proximity of the -10 or -30/35 element in bacterial promoter regions.

To confirm that the presence of methylation close to the -10 or -30/35 element influences transcription and therefore gene expression in *B. cenocepacia*, translational eGFP reporter fusions were constructed and eGFP production was quantified. The eGFP production in strains harboring different plasmids is shown in Figure 7. As expected, the production of eGFP, driven by the promoters of genes BCAL1515, BCAM0820, and BCAL0079, was significantly ($p = 0.001$, $p = 0.014$, $p = 0.002$, respectively) increased in the deletion mutant for which an upregulation of these genes was observed using qPCR experiments (Figure 7).

DNA methylation in the origin of replication

DNA methylation was detected in all origins of replication of *B. cenocepacia* (Figure 8). Similar methylation patterns were observed in the origins of the different replicons. A previously discovered 7-mer (CTGTGCA) that can be found in all

replication origins (30), contains a CACAG methylation motif on the antisense strand. This motif was also found at the 3'-end of almost every DnaA box. These boxes are bound by DnaA proteins, essential for DNA unwinding and chromosome replication initiation (31). Also, the GTWWAC motif was found in proximity of the replication origins, consequently the origins in *B. cenocepacia* represent methylation-rich regions. Whereas methylated CACAG motifs were found throughout the origins of replication, the position of the GTWWAC methylation was unique in all replicons and at least two GTWWAC motifs were found in between two CACAG methylated DnaA boxes. In contrast to the origins of the three larger replicons, the origin of replication of the plasmid contained only one CACAG methylated DnaA box.

Discussion

Despite the growing knowledge of DNA methylation in prokaryotes (15), the role of DNA MTases in regulating gene expression in *B. cenocepacia* remains to be revealed. In the present study, we identified two DNA MTases (BCAL3494 and BCAM0992), and mutants in which these genes were deleted, showed differences in biofilm formation and motility. In addition, when methylation was blocked by the DNA MTase inhibitor sinefungin (32), the same phenotypic differences were observed. These findings demonstrate that epigenetic control of gene expression by MTases play an important role in controlling certain phenotypes. Similar results have been reported in *Salmonella enterica*, where DNA methylation is crucial for optimal pellicle and biofilm production (33).

Methylome analysis showed that mutants in which MTase ΔBCAL3494 or ΔBCAM0992 were inactivated, lacked adenine methylation in specific motifs. MTase

BCAL3494 was specifically linked to methylation of the CACAG motif, MTase BCAM0992 to methylation of the GTWWAC motif. This strategy of DNA methylation analysis, in which the methylome of strains lacking MTases is determined, has been used in various bacteria, as it is an effective way to find associations between predicted MTases and genome-wide methylation motifs (34,35). For example, several methylation motifs were identified in *Burkholderia pseudomallei*, including motifs CACAG and GTWWAC (36). Two of the *B. pseudomallei* MTases (M.BpsI and M.BpsII) are homologous to the *B. cenocepacia* MTases BCAL3494 and BCAM0992. In *Ralstonia solanacearum*, an important plant pathogen that is phylogenetically related to *B. cenocepacia*, the GTWWAC methylation motif co-occurs with the respective homolog of the BCAM0992 MTase, whereas a BCAL3494 MTase homolog and methylation of CACAG are absent (37). As in *B. cenocepacia*, the BCAM0992 homolog in *R. solanacearum* is an orphan DNA MTase. Analysis of cytosine methylation suggests that cytosine is more likely to be methylated at random instead of at specific motifs, and is likely not having a major regulatory function. Also, GC-rich genomes complicate the search for specific cytosine motifs.

Previous epigenetic research demonstrated that there is a negative correlation between methylation in promoters and transcription (38). To uncover the role of DNA methylation in regulation of *B. cenocepacia* gene expression, all methylated motifs in promoter regions were identified. The data obtained in the present study indicates that gene expression was upregulated in DNA MTase mutants, suggesting that adenine DNA methylation in *B. cenocepacia* affects gene expression by a mechanism inhibiting transcription. In both prokaryotes and eukaryotes, adenine and cytosine methylation are

involved in blocking (or enhancing) the binding of RNA polymerase to DNA (15,21,39), and especially methylation near the -10 and -30/35 elements in the promoter region seems to be important for affecting RNA polymerase binding (40). We found that, also in *B. cenocepacia*, methylated motifs (CACAG and GTWWAC) are found close to, or in these elements.

BCAM0820, upregulated in the J2315 and K56-2 ΔBCAL3494 mutant, is a two-component response regulator, the first gene of an operon homologous to the Wsp chemosensory system involved in biofilm formation in *Pseudomonas aeruginosa* (41). BCAM0820 is homologous to WspR, but lacks the diguanylate cyclase domain. During an experimental evolution study in which *B. cenocepacia* HI2424 biofilms were grown on beads, mutations within the *wsp* gene cluster occurred in different clones; these were associated with increased pellicle formation and increased biofilm formation on beads. This demonstrates that the Wsp cluster is involved in pellicle formation in *B. cenocepacia* (42,43), and the upregulation of BCAM0820 could explain the differences in pellicle and biofilm formation between the wild type strains and the ΔBCAL3494 deletion mutants observed in the present study. Interestingly, BCAL1515, encoding 2-oxoglutarate dehydrogenase (SucA) and upregulated in ΔBCAL3494, also acquired mutations in the course of the experimental evolution study (43), but the role of this gene in biofilm formation has not been further explored. BCAL0079, upregulated in the ΔBCAM0992 mutants, is annotated as a DNA helicase gene (*rep*). Besides unwinding DNA during DNA replication, Rep plays a role in swimming motility in *E. coli* (44). The reduced motility observed in the ΔBCAM0992 mutants suggests that Rep may also affect motility in *B. cenocepacia*, although this remains to be confirmed.

295 Measurement of eGFP production in translational fusion mutants revealed that
296 mutants with constructs containing the BCAL1515, BCAM0820, or BCAL0079 promoter,
297 showed a significant increase in eGFP production compared to wild type, thereby
298 supporting our hypothesis of gene expression regulation by DNA methylation. *In silico*
299 analyses predict that sequences containing methylation motifs are similar to binding
300 sites of TF in *E. coli* K12, and it is plausible that these sequences are also part of TF
301 binding sites in *B. cenocepacia*, allowing us to propose a possible mechanism of gene
302 expression regulation (Figure 9). TFs that bind close to the -10 and -35 region often act
303 as transcriptional repressors (45). Therefore, a methylated promoter region could
304 promote binding of a repressor (46), and sterically hinder RNA polymerase (OFF state),
305 whereas an absence of methylation would allow binding of the initiation factor sigma to
306 the promoter, which in turn could lead to binding of RNA polymerase and initiation of
307 transcription (ON state).

308 The role of DNA methylation in prokaryotes in multifaceted. Besides gene
309 expression regulation and a role in DNA mismatch repair in Gram-positive bacteria (47),
310 DNA methylation has also been implicated in the coordination of replication initiation.
311 Results of the present study seem to confirm this, as the *rep* gene, necessary for
312 replication, was found to be under epigenetic control by DNA methylation. In *E. coli*,
313 GATC motifs, omnipresent in the replication origin, are prone to adenine methylation.
314 The motifs are found within DnaA boxes, essential for binding of the DnaA protein and
315 initiation of replication. The methylation state of each of these GATC motifs changes the
316 affinity of DnaA and sequestering-protein SeqA for the DnaA box. Immediately after
317 replication, GATC motifs are hemi-methylated, which leads to sequestration of the DnaA

boxes by SeqA and prevents the process of replication to be reinitiated (21). The occurrence of methylated motifs in the vicinity of the origins of replication of the four replicons in *B. cenocepacia* was studied to check for a link between DNA methylation and coordination of the replication process. An enrichment of the CACAG motif was observed in the origin of replication of all replicons. The motif was found to be part of a bigger sequence that has previously been reported as a recurring 7-mer (30), without known function. In addition, the origin of replication of the different replicons showed high similarities in methylation patterns, raising the possibility of replication coordination by DNA methylation.

In conclusion, we have demonstrated that DNA methylation plays a role in regulation of gene expression in *B. cenocepacia*. DNA MTases BCAL3494 and BCAM0992 are essential for methylation of the *B. cenocepacia* genome, and are responsible for methylation of base motifs CACAG and GTWWAC, respectively. In absence of methylation, expression of certain genes in affected and this results in altered phenotypes (including cell clustering, biofilm formation, and motility). Finally, recurrent methylation patterns were detected in all origins of replication, which suggests an additional role of DNA methylation in replication regulation.

Materials and Methods

Strains and culture conditions

All strains and plasmids used in this study are listed in Table 3. *B. cenocepacia* strains were cultivated in phosphate buffered mineral medium (2.00 g/L NH_4Cl, 4.25 g/L $K_2HPO_4.3H_2O$ (ChemLab), 1.00 g/L $NaH_2PO_4.H_2O$, 0.10 g/L nitriloacetic acid, 0.0030 g/L $MnSO_4.H_2O$, 0.0030 g/L $ZnSO_4.7H_2O$, 0.0010 g/L $CoSO_4.7H_2O$, 0.20 g/L

$MgSO_4.7H_2O$, 0.012 g/L $FeSO_4.7H_2O$ (Sigma-Aldrich), 5 g/L Yeast Extract (Lab M), 2 g/L Casamino Acids (BD Biosciences), and 5 g/L glycerol (Scharlab)). LB medium (Luria Bertani medium with 5g/L NaCl, Sigma-Aldrich) was used for maintenance of *E. coli* strains and during specific stages of the gene deletion procedure (see below) where antibiotic selection with tetracycline (250 µg/mL) (Sigma-Aldrich) was desired. Prior to phenotypic experiments, liquid overnight (ON) cultures were grown in a shaker incubator (100 rpm) at 37 °C.

Selection of DNA MTase genes – *in silico*

The REBASE Genome database was used to allocate all known DNA MTase genes in the *B. cenocepacia* J2315 and K56-2 genomes (48). The Artemis Genome Browser and Annotation Tool (Sanger) allowed to visualize the genomic context of these genes (49). NCBI BLAST was used to screen for conservation of the genes within the *Burkholderia* genus using default search parameters (50) (search mode: BLASTn, E cut-off value: < 1E-5).

Construction of deletion mutants

All primers used for construction and complementation of the deletion mutants are listed in Table S6. The procedure is an adapted allelic replacement approach, using a suicide plasmid with a SceI endonuclease recognition site (51,52). The suicide plasmid, containing DNA fragments of regions flanking the target gene, is integrated into the *B. cenocepacia* genome by homologous recombination. Introducing a second plasmid that carries SceI endonuclease genes into *B. cenocepacia*, results in a lethal genomic strand break. Another homologous recombination event allows the bacteria to repair the break with a 50 % chance of resulting in a gene deletion. Deletion mutants

ΔBCAL3494 and ΔBCAM0992 were constructed in both *B. cenocepacia* J2315 and K56-2.

BCAL3494 was deleted together with neighboring gene BCAL3493, as well as BCAL3488 to BCAL3492 (encoding hypothetical proteins). Targeting BCAL3494 alone was not feasible because regions flanking BCAL3494 contain multiple recognition sites for endonucleases used during construction of the deletion mutants, and digestion of these regions would be inevitable (Figure S1).

E. coli One Shot PIR2 cells (Thermo Fisher), expressing λ *pir*, were used for transformation, replication, and maintenance of the suicide plasmid during construction of deletion mutants. Thawed cells were immediately exposed to a heat shock transformation procedure, after which they were transferred to SOC medium for recovery. For plasmid selection, the phosphate buffered mineral medium was supplemented with one or more of following antibiotics: trimethoprim (Ludeco; 50 µg/mL for initial screening in *E. coli*, 200 µg/mL when plasmid is introduced in *B. cenocepacia*), chloramphenicol (400 µg/mL), gentamicin (50 µg/mL), kanamycin (50 µg/mL), and ampicillin (200 µg/mL) (Sigma-Aldrich).

Construction of plasmids for complementation

To ensure that phenotypes were solely caused by the deletion of DNA MTases, deletion mutants were complemented. The primers used for construction of plasmids used for complementation are listed in Table S6. Plasmids pJH2 and pSCrhaB2 were used for complementation of ΔBCAL3494 (*c*ΔBCAL3494) and ΔBCAM0992 (*c*ΔBCAM0992), respectively. The genomic sequences of the DNA MTase genes were PCR-amplified and subsequently cloned into the plasmids. BCAL3494 was amplified

387 including its own regulatory region (approx. 250 nucleotides upstream of the
388 transcription start site) into pJH2, which does not have a promoter associated with its
389 multiple cloning site (53). BCAM0992 does not have its own upstream promoter,
390 therefore it was cloned into pSCrhaB2, which contains a rhamnose-inducible promoter
391 (54). Complemented mutant strains were subjected to the same phenotypic tests as the
392 deletion mutants and wild type *B. cenocepacia*. For strains *c*ΔBCAM0992, the
393 phosphate buffered mineral medium was supplemented with 0.2 % rhamnose.

394 **Biofilm and clustering experiments**

395 Biofilms were grown in plastic U-shaped 96-well microtiter plates in phosphate
396 buffered medium at 37 °C, starting from 200 µL/well planktonic overnight cultures with
397 an optical density (OD) of 0.05 (590 nm). After 4 h static incubation, all wells were
398 rinsed with physiological saline (PS, 0.9 % NaCl in water), thereby removing all
399 unattached planktonic cells. Wells were re-filled with 200 µL medium and incubated for
400 an additional 20 h. Where appropriate, biofilms were stained with LIVE/DEAD
401 (SYTO9/propidium iodide, Invitrogen) to visualize the bacteria and distinguish live and
402 dead cells (55). Pellicle formation was determined in glass tubes. Cultures were grown
403 statically for 24 h, after which adhering pellicles were stained and quantified with crystal
404 violet (56). Cell clustering, already shown to be correlated with pellicle formation, was
405 determined with flow cytometry (Attune NxT Flow Cytometer, Thermo Fisher) (57).
406 Forward scatter (FCS), a value for particle size, and side scatter (SSC), a value for
407 particle complexity, were measured for each particle present in the bacterial suspension
408 and visualized in scatter plots. After analysis of these graphs, the main cell population

was gated (gate ranging from approx. 10^3 to 10^5 for both FSC and SSC), and detected events larger and more complex than the gate, were considered clustered (Figure S6).

Motility experiments

Petri dishes containing phosphate buffered mineral medium with agar concentrations of 0.3 % and 0.5 % were used for assessment of swimming and swarming motility, respectively. 1 µL of cultures with OD 0.1 was spotted on the agar plates. Diameters were measured after 24 h (strain K56-2) or 32 h (strain J2315).

DNA MTase inhibition with sinefungin

A stock solution of the DNA MTase inhibitor sinefungin (Sigma-Aldrich) was prepared (10 mg/mL) (29), aliquoted, and immediately frozen at -20 °C to prevent degradation. Cells were grown for 24 h in sinefungin-supplemented medium (50 µg/mL) and used as inoculum for an overnight culture, also in sinefungin supplemented medium. This allowed the DNA MTase inhibitor to have an effect during several growth cycles. Then, biofilm formation and motility of sinefungin-treated cells was assessed as described above in medium supplemented with 50 µg/mL sinefungin.

Genomic DNA extraction

Prior to DNA extraction, planktonic strains were grown overnight in a shaker incubator (100 rpm) at 37 °C. Biofilm cells were grown as described above. Next, cells were harvested and genomic DNA (gDNA) was extracted using the Wizard Genomic DNA Purification Kit (Promega). Quantification was performed with a BioDrop µLITE (BioDrop) spectrophotometer.

SMRT sequencing

To determine the methylome of *B. cenocepacia*, gDNA extracts were analyzed with Single Molecule Real-Time (SMRT) Sequencing technology. gDNA samples of both wild type and mutant strains were run on a Pacific Biosciences Sequel System (250x coverage) according to the manufacturer's guidelines. Library preparations were multiplexed as data output of approximately 2 Gb per genome was expected, and a single SMRT Sequel cell provides up to 6 Gb data. Initial data output was processed with SMRT Link software (Pacific Biosciences). Identification of the modified bases and analysis of the methylated motifs was performed with the Base Modification and Motif Analysis application (SMRT Link v6.0, Pacific Biosciences). In depth data analysis was performed with CLC Workbench Genomics (v11.0.1, Qiagen). Differential analysis between wild type and mutants was performed to identify methylation motifs specifically associated with certain DNA MTases. Previously predicted promoter regions and transcription start sites of *B. cenocepacia* were used to determine the methylation profile of regulatory regions (58). Virtual Footprint software (promoter analysis mode, default search parameters) was used to assess similarity of the methylation motifs to known TF binding sites (59).

qPCR

To evaluate the impact of DNA methylation in promoter regions on gene expression, qPCR was performed on all genes that had a methylated promoter region in wild type *B. cenocepacia*, but an absence of methylation in promoter region in one of the deletion mutants. All hypothetical genes and genes with unknown function, as well as genes with low innate expression level, were excluded from testing. The primers

453 used for qPCR are listed in Table S7. First, all strains were grown to an OD of 0.6 in
454 phosphate buffered medium, after which they were pelleted by centrifugation and frozen
455 at -80 °C. Next, RNA was extracted using the RiboPure – Bacteria extraction kit
456 (Invitrogen), followed by a DNase treatment to remove trace quantities of gDNA.
457 Quantification and measurement of RNA purity of the extracts was performed with a
458 BioDrop µLITE (BioDrop). Subsequently, cDNA was synthesized, using 500 ng RNA per
459 reaction, with a Reverse Transcriptase kit (High-Capacity cDNA RT Kit, Applied
460 Biosystems). Per qPCR reaction, 2 µL template cDNA was mixed with 10 µL GoTaq
461 qPCR Master Mix, 0.6 µL qPCR primer mix (10 µg/mL), and 7.4 µL nuclease-free water
462 according to the GoTaq qPCR Master Mix (Promega) protocol. Samples were run on a
463 CFX96 Real-Time System C1000 Thermal Cycler (Bio-Rad) and output data was
464 processed with Bio-Rad CFX Manager 3.1 software. The baseline threshold was set to
465 a defined 100 RFU. Obtained Cq values were normalized to reference gene *rpo*D
466 (BCAM0918) of which the expression was stable across all samples, differences to wild
467 type were calculated (ΔΔCq) and log-transformed. Volcano plots were used to plot the
468 negative logarithm of statistical p-values against log 2-fold changes (Figure S5).

469 **Construction of translational eGFP reporter fusions and measurement of eGFP**
470 **production**

471 Genes with methylated promoter regions that showed a significant upregulation
472 of gene expression in one of both mutant strains, were selected for eGFP experiments.
473 Translational eGFP reporter fusion plasmids were constructed by cloning the regulatory
474 regions of the genes, comprising 60 to 390 nucleotides upstream of the transcription
475 start site, into vector pJH2. The insert is cloned right in front of the eGFP gene and

contains an ATG start codon at the 3'-end, in frame with the codon sequence of the gene. All primers used for amplification of the regulatory regions and screening of pJH2 with correct insert length, are listed in Table S8. The plasmids were transferred to *B. cenocepacia* J2315 and K56-2 by triparental mating. Exconjugants were grown on selective plates (LB medium supplemented with 200 µg/mL chloramphenicol and 50 µg/mL gentamicin) and PCR-screened to confirm the presence of the insert. Constructs carrying genes BCAL2415, BCAL2465 and BCAM1362 repeatedly failed to be transformed into *B. cenocepacia* and were not included in further experiments. Fluorescent signals of eGFP production in wild type and mutant strains were measured by flow cytometry (Attune NxT Flow Cytometer, Thermo Fisher) (53).

Data analysis and statistics

Statistical analysis was performed using SPSS Statistics v. 25 software. All tests and experiments were run in triplicate unless otherwise mentioned. Normality of data was verified with a Shapiro-Wilk test. To check for significant differences between data, normally distributed data was subjected to a T-test or One-way ANOVA test, not normally distributed data to a non-parametric Mann-Whitney U-test. Resulting p-values smaller than 0.05 were reported as statistically significant.

Acknowledgements

This work was funded by the Special Research Fund of Ghent University (Bijzonder Onderzoeksfonds, BOF, grant number BOFDOC2016001301) and the Swiss National Science Foundation (31003A_169307).

Figures

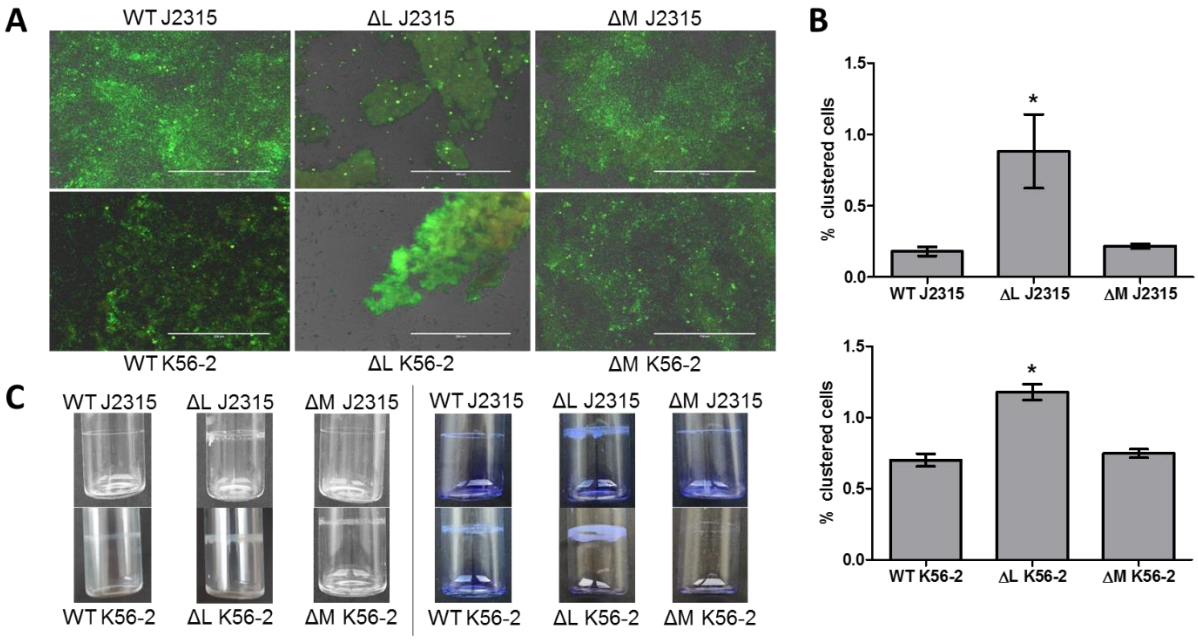

FIGURE 1 Effect of DNA MTase deletion on biofilm structure, cell aggregation, and pellicle formation in *B. cenocepacia* J2315 and K56-2. (A) Microscopic images of LIVE/DEAD stained biofilms, grown in microtiter plate wells for 24 h. White bar (200 µm) for scale. (B) Clustering of cells in planktonic cultures, quantified with flow cytometry. (C) Pellicle formation inside glass tubes after 24 h of static incubation. Left pictures represent unstained samples, right pictures display pellicles stained with crystal violet. (n=3, * $p < 0.05$ compared to wild type, error bars represent the standard error of the mean (SEM)). WT: wild type, ΔL: deletion mutant ΔBCAL3494, ΔM: deletion mutant ΔBCAM0992)

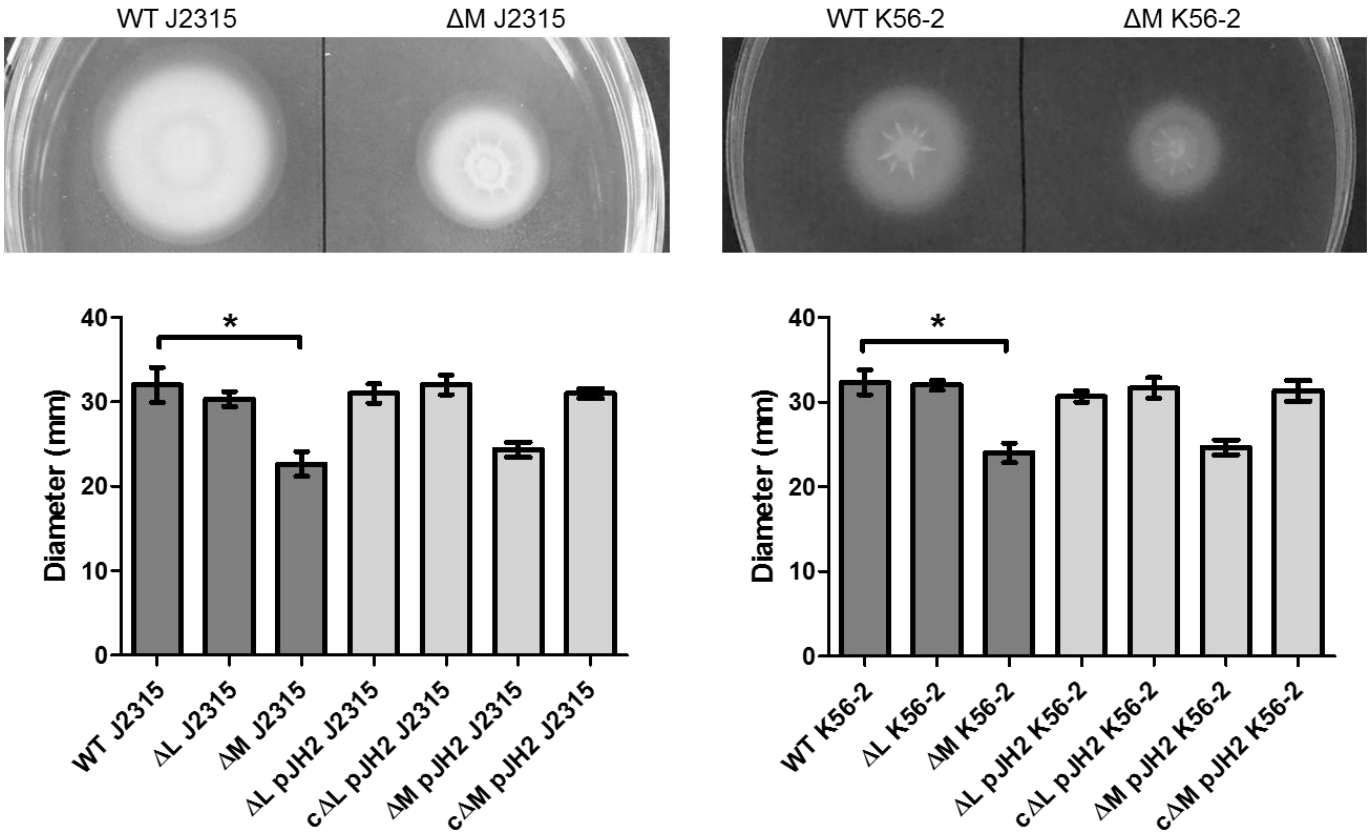

FIGURE 2 Swimming motility of DNA MTase deletion mutants. Diameters were measured after 24 h (K56-2) or 32 h (J2315). (n=3, * $p < 0.05$ compared to wild type, error bars represent the SEM. WT: wild type, ΔL: deletion mutant ΔBCAL3494, ΔM: deletion mutant ΔBCAM0992, ΔL pJH2 and ΔM pJH2: mutant strains with empty vector pJH2 (vector control), *c*ΔL pJH2 and *c*ΔM pJH2: deletion mutants complemented with genes BCAL3494 and BCAM0992)

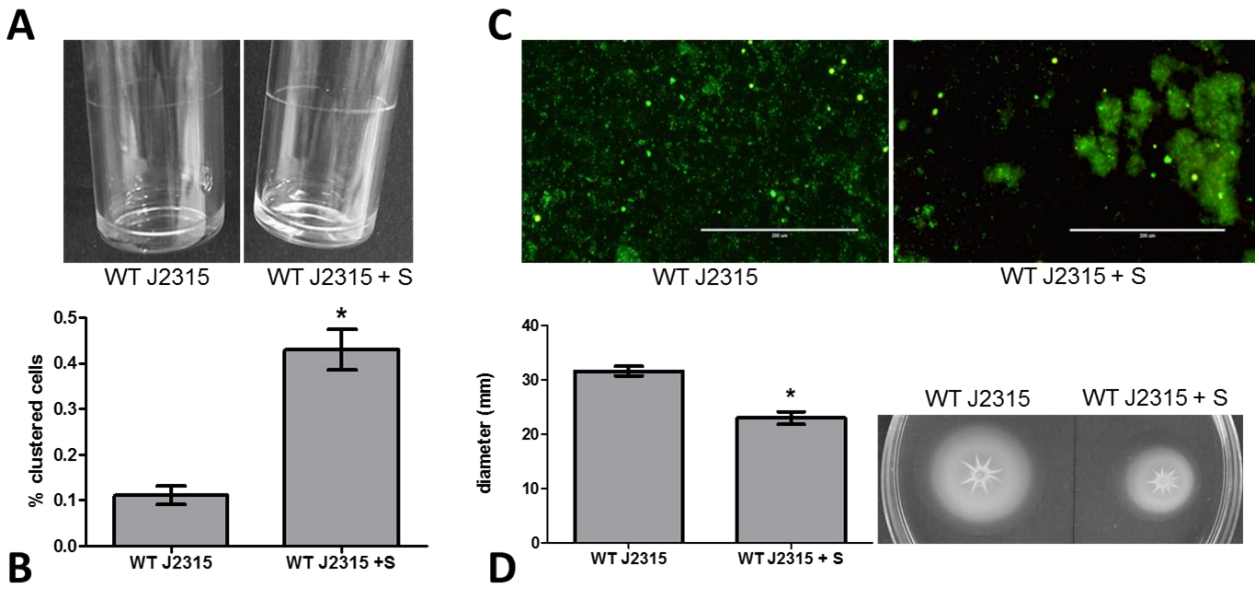

FIGURE 3 Effect of DNA MTase inhibitor sinefungin on biofilm and pellicle formation, cell aggregation and motility. (A) Pellicle formation inside glass tubes after 24 h of static incubation. (B) Clustering of planktonic cultures analyzed with flow cytometry. (C) Microscopic images of LIVE/DEAD stained biofilms, grown on plastic surfaces in microtiter plates for 24 h. (D) Swimming motility of treated and untreated samples. (n=3, * $p < 0.05$ compared to wild type, error bars represent the SEM). WT: wild type, +S: medium supplemented with 50 µg/mL sinefungin)

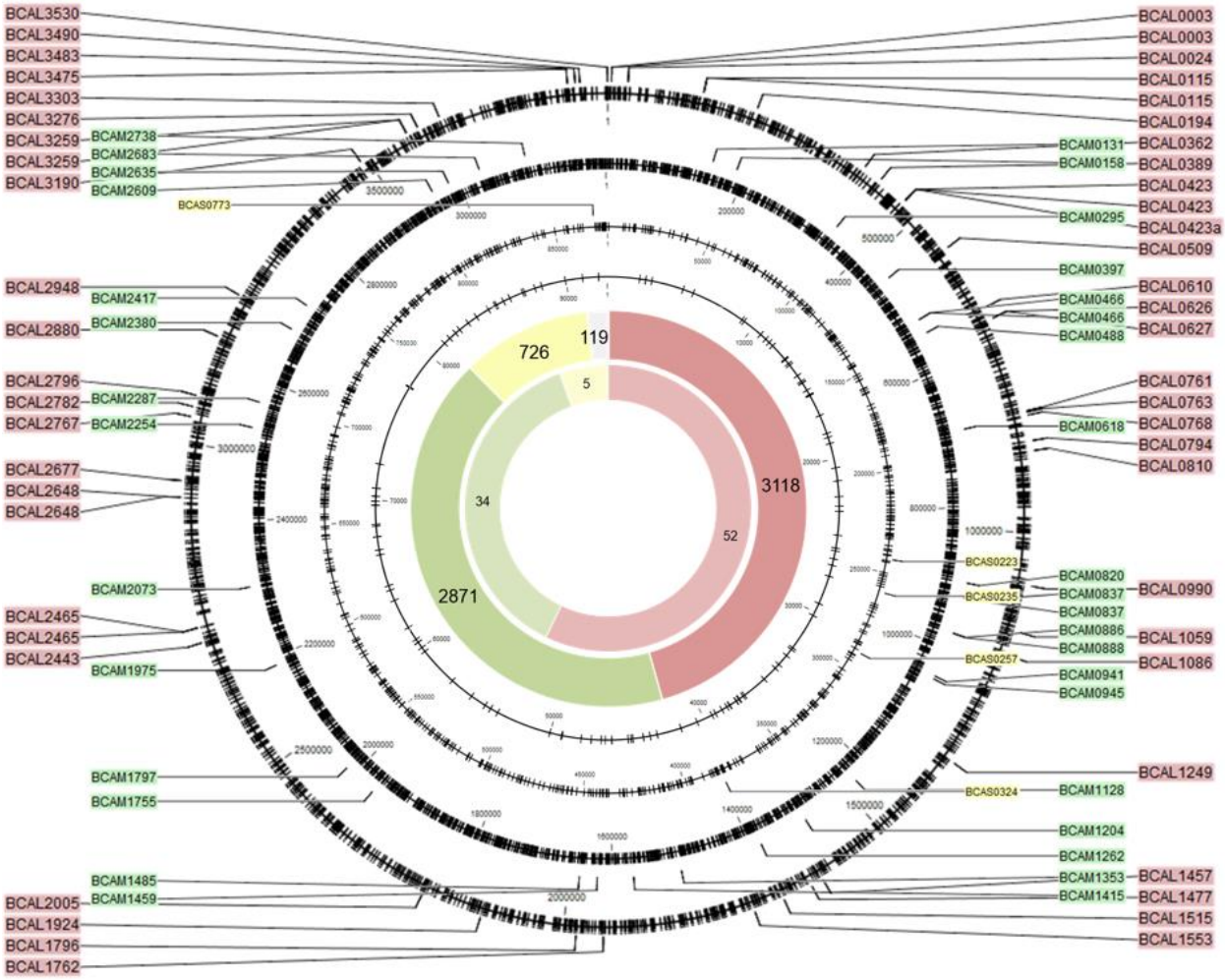

FIGURE 4 Genomic position of all methylated CACAG motifs. Black circles represent the four replicons of *B. cenocepacia*, black ticks mark the motif locations. The total number of methylated CACAG motifs and methylated CACAG motifs in promoter regions, per replicon (red: replicon 1, green: replicon 2, yellow: replicon 3, and grey: plasmid), is shown on the large and small inner circle, respectively. The position and names of genes with methylated promoter regions is indicated with colored labels (same color code).

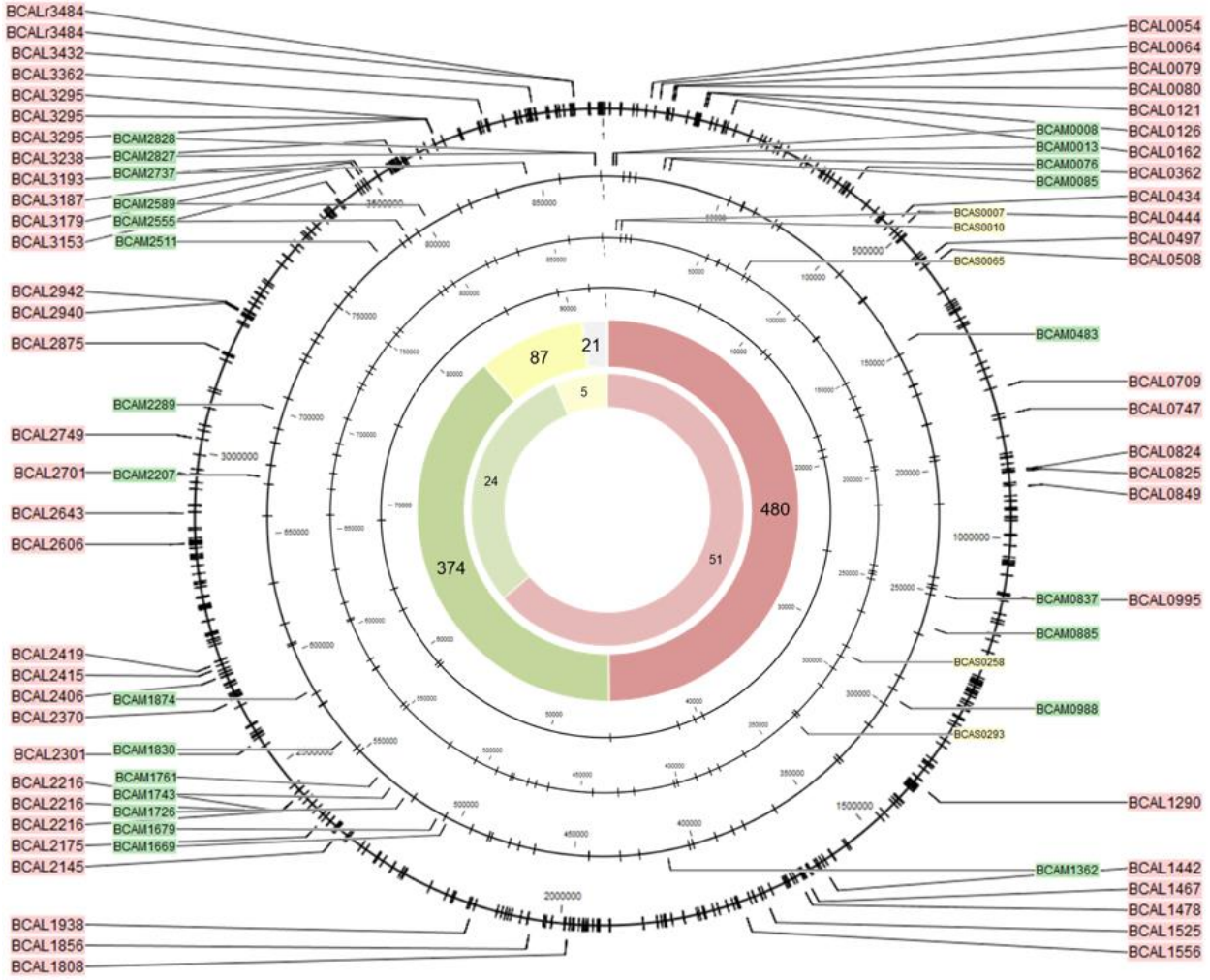

FIGURE 5 Genomic position of all methylated GTWWAC motifs. Black circles represent the four replicons of *B. cenocepacia*, black ticks mark the motif locations. The total number of methylated GTWWAC motifs and methylated GTWWAC motifs in promoter regions, per replicon (red: replicon 1, green: replicon 2, yellow: replicon 3, and grey: plasmid), is shown on the large and small inner circle, respectively. The position and names of genes with methylated promoter regions is indicated with colored labels (same color code).

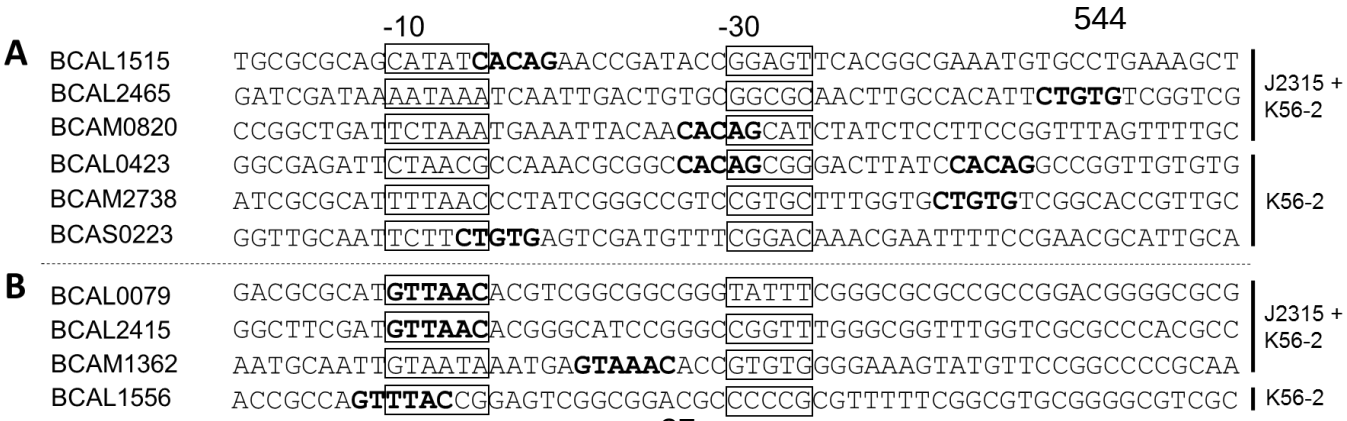

FIGURE 6 Position of methylated motifs relative to gene start for genes of which the expression is upregulated in DNA MTase deletion mutants. (A) Genes with methylated CACAG motifs in their corresponding promoter region. (B) Genes with methylated GTWWAC motifs in their corresponding promoter region. The motifs are marked in bold, the position of -10 and -30/35 elements in bacterial promoters are framed. ('J2315 + K56-2': upregulation in both strains, 'K56-2': upregulation in strain K56-2 only)

551

552

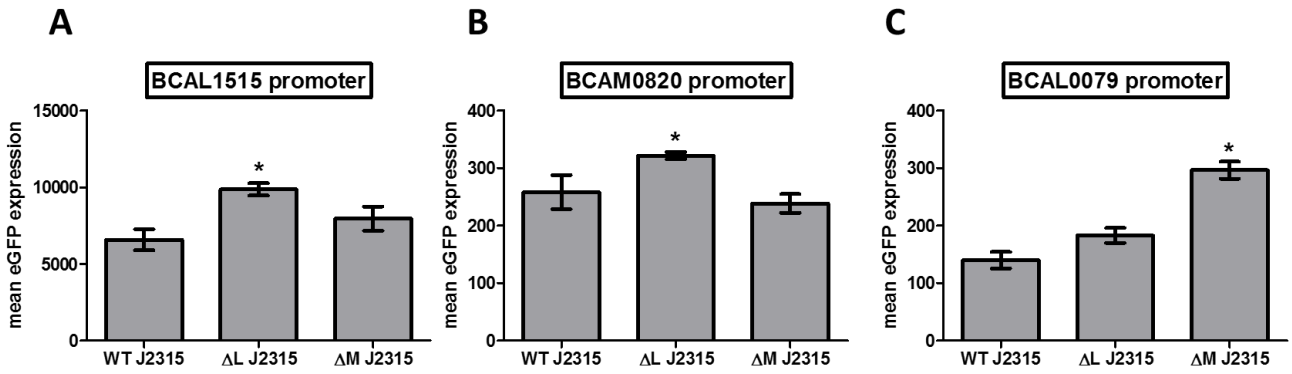

553

554 **FIGURE 7** eGFP production in *B. cenocepacia* J2315 strains harboring a pJH2 plasmid
555 that contains a BCAL1515 promoter-eGFP construct (A), a BCAM0820 promoter-eGFP
556 construct (B), or a BCAL0079 promoter-eGFP construct (C). BCAL 1515 and
557 BCAM0820 are associated with methylation of the CACAG motif by DNA MTase
558 BCAL3494, BCAL0079 is associated with methylation of the GTWWAC motif by DNA
559 MTase BCAL0992 (n=3, * $p < 0.05$ compared to wild type, error bars represent the
560 SEM). WT: wild type, ΔL: deletion mutant ΔBCAL3494, ΔM: deletion mutant
561 ΔBCAM0992).

562

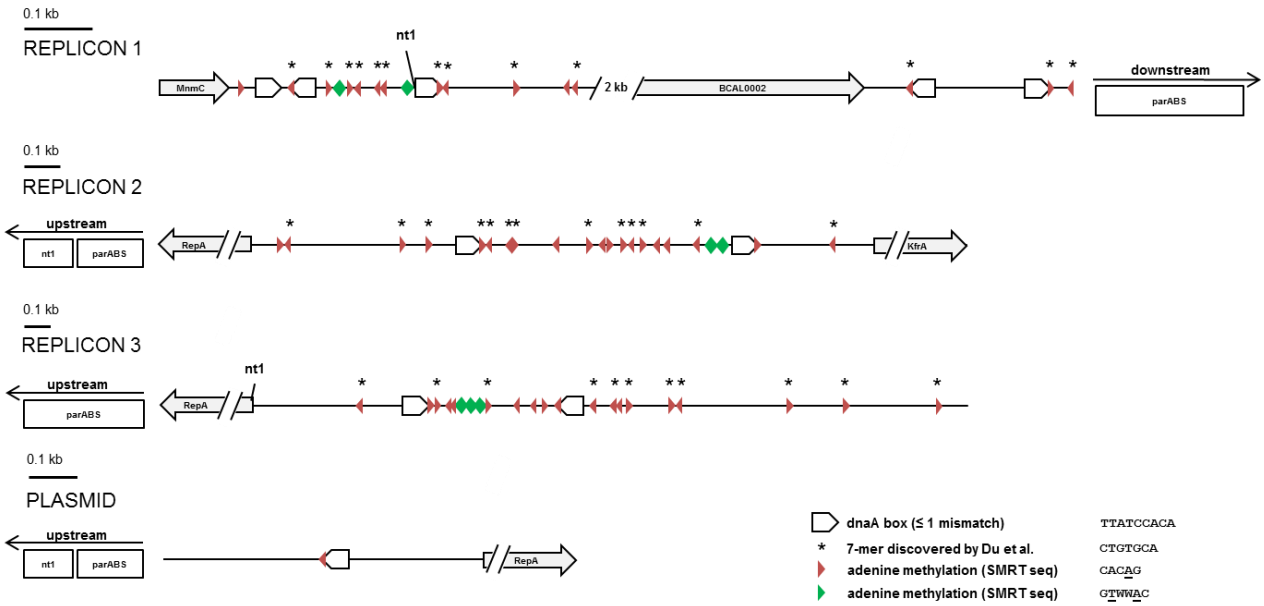

563

564 **FIGURE 8** Methylation in the origin of replication of the different replicons in
565 *B. cenocepacia* J2315. SMRT sequencing was used to detect methylated CACAG (red
566 triangles) and GTWWAC (green triangles) motifs within these regions. DnaA boxes
567 (TTATCCACA, consensus sequence of DnaA boxes in *E. coli*) are indicated in the
568 figure. CACAG motifs were frequently found to be part of a previously discovered 7-mer
569 (sense: CTGTGCA, antisense: TGCACAG) (30). The positions of these 7-mers are
570 indicated with an asterisk. (nt1, nucleotide 1; parABS genes, responsible for
571 chromosome segregation in *B. cenocepacia*)

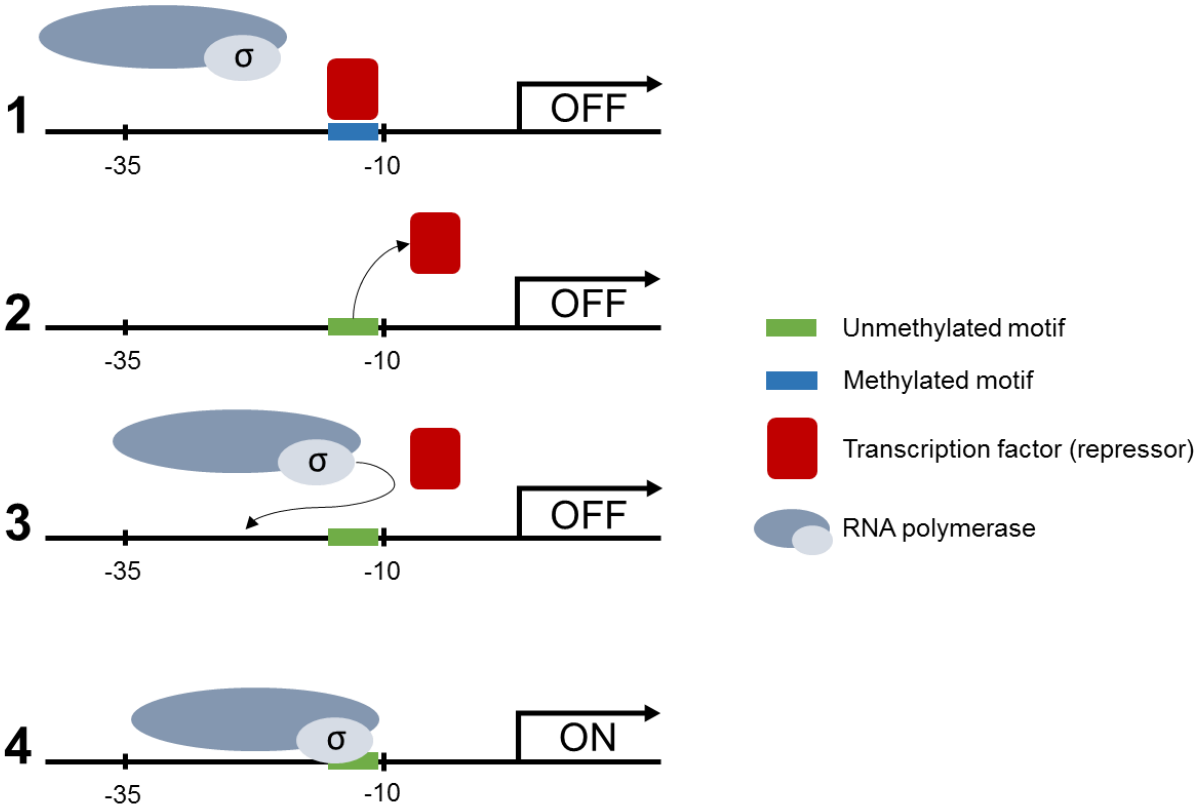

572

573 **FIGURE 9** Proposed mechanism of regulation of gene expression in *B. cenocepacia*.
574 (1) Methylated motifs in the promoter region of the gene are bound by a TF, acting as
575 repressor (OFF state). (2) In absence of methylation in the promoter region, the TF
576 dissociates from the motif and vacates the promoter region. (3) The sigma factor is no
577 longer sterically hindered by a repressor and is able to bind to the promoter region. (4)
578 RNA polymerase can access the promoter region and start transcription of the gene
579 (ON state).

580

581

Tables

TABLE 1 Expression changes of genes with a methylated CACAG motif in their promoter region in deletion mutants compared to wild type.

Locus tag	J2315		K56-2		Gene function
	Fold change	p-value	Fold change	p-value	
BCAL0003	0.954	0.791	1.242	0.214	MarR family regulatory protein
BCAL0024	1.477	0.143	0.909	0.678	GidA tRNA uridine 5-carboxymethylaminomethyl modification enzyme
BCAL0423	1.169	0.306	1.948	0.014	DnaA chromosomal replication initiation protein
BCAL0509	1.129	0.473	1.175	0.199	MetK S-adenosylmethionine synthetase
BCAL1059	1.129	0.662	0.767	0.457	ArgD bifunctional N-succinyldiaminopimelate-aminotransferase/acetylornithine transaminase protein
BCAL1457	1.343	0.309	1.793	0.056	LysR family regulatory protein
BCAL1515	1.790	0.032	1.869	0.012	SucA 2-oxoglutarate dehydrogenase E1 component
BCAL2465	1.277	0.047	2.042	0.014	TetR family regulatory protein
BCAL2767	1.281	0.270	1.397	0.382	ArgF ornithine carbamoyltransferase
BCAL2782	1.373	0.237	1.166	0.668	PdxH pyridoxamine 5'-phosphate oxidase
BCAL3303	1.048	0.845	1.093	0.071	QueA S-adenosylmethionine:tRNA ribosyltransferase-isomerase
BCAM0820	2.621	0.004	2.253	0.002	hybrid two-component system kinase-response regulator protein
BCAM0941	1.240	0.448	1.761	0.050	*gnd* 6-phosphogluconate dehydrogenase
BCAM1262	1.237	0.397	1.163	0.445	dihydroxy-acid dehydratase
BCAM1415	1.183	0.665	1.315	0.177	AraC family regulatory protein
BCAM2738	1.213	0.147	1.649	0.022	IspH 4-hydroxy-3-methylbut-2-enyl diphosphate reductase
BCAS0223	1.251	0.202	1.993	0.030	AfcC fatty acid desaturase

587 **TABLE 2** Expression changes of genes with a methylated GTWWAC motif in their
588 promoter region in deletion mutants compared to wild type.

Locus tag	J2315		K56-2		Gene function
	Fold change	p-value	Fold change	p-value	
BCAL0054	0.487	0.127	0.641	0.107	MerR family regulatory protein
BCAL0079	2.838	0.020	3.074	0.005	*rep* ATP-dependent DNA helicase
BCAL0126	0.845	0.356	0.801	0.607	MotA chemotaxis protein
BCAL0162	0.139	0.634	0.133	0.478	GmhA phosphoheptose isomerase
BCAL0508	1.015	0.934	1.721	0.137	LpxL lipid A biosynthesis myristoyl acyltransferase
BCAL0709	1.599	0.104	0.763	0.430	LipB lipoate-protein ligase B
BCAL1556	1.611	0.171	1.690	0.006	RpiA ribose-5-phosphate isomerase A
BCAL2406	1.693	0.273	1.009	0.938	WabR putative glycosyltransferase
BCAL2415	2.819	0.006	6.029	0.001	PurT phosphoribosylglycinamide formyltransferase 2
BCAL2701	0.613	0.076	1.519	0.170	ArgD acetylornithine transaminase protein
BCAL2942	1.143	0.474	1.451	0.274	CysM cysteine synthase B
BCAM0076	1.630	0.112	1.358	0.051	TetR family regulatory protein
BCAM1362	1.959	0.025	1.516	0.004	putative penicillin-binding protein
BCAS0258	1.247	0.451	1.141	0.438	GntR family regulatory protein

589

590

591 **TABLE 3** Bacterial strains and plasmids.

Strain/Plasmid	Description	Abbreviation	Source
B. cenocepacia			
J2315	CF sputum isolate	WT J2315	LMG16656
J2315 ΔBCAL3494	BCAL3494 MTase deletion mutant	ΔL J2315	this study
J2315 ΔBCAM0992	BCAM0992 MTase deletion mutant	ΔM J2315	this study
J2315 ΔBCAL3494 pJH2	BCAL3494 MTase mutant with empty pJH2 vector	ΔL pJH2 J2315	this study
J2315 ΔBCAL3494 pJH2 + BCAL3494	BCAL3494 MTase complemented deletion mutant	*c*ΔL pJH2 J2315	this study
J2315 ΔBCAM0992 pJH2	BCAM0992 MTase mutant with empty pJH2 vector	ΔM pJH2 J2315	this study
J2315 ΔBCAM0992 pJH2 + BCAM0992	BCAM0992 MTase complemented deletion mutant	*c*ΔM pJH2 J2315	this study
K56-2	CF sputum isolate	WT K56-2	LMG 18863
K56-2 ΔBCAL3494	BCAL3494 MTase deletion mutant	ΔL K56-2	this study
K56-2 ΔBCAM0992	BCAM0992 MTase deletion mutant	ΔM K56-2	this study
K56-2 ΔBCAL3494 pJH2	BCAL3494 MTase mutant with empty pJH2 vector	ΔL pJH2 K56-2	this study
K56-2 ΔBCAL3494 pJH2 + BCAL3494	BCAL3494 MTase complemented deletion mutant	*c*ΔL pJH2 K56-2	this study
K56-2 ΔBCAM0992 pJH2	BCAM0992 MTase mutant with empty pJH2 vector	ΔM pJH2 K56-2	this study
K56-2 ΔBCAM0992 pJH2 + BCAM0992	BCAM0992 MTase complemented deletion mutant	*c*ΔM pJH2 K56-2	this study
E. coli			
DH5α	Maintenance of replicative plasmids		lab stock
One Shot PIR2	Maintenance of suicide plasmids with ori_{R6K}	PIR2	ThermoFisher
Plasmids			
pGPI-SceI-XCm	Suicide plasmid, Tp^r, Cm^r, I-SceI restriction site, ori_{R6K}	pGPI	44,45
pDAI-SceI-SacB	Replicative plasmid, Tet^r, I-SceI nuclease, counterselectable marker SacB, ori_{pBBR1}	pDAI	44,45
pRK2013	Helper plasmid, Km^r, ori_{colEI}	pRK	44,45
pJH2	Broad-range translational fusion vector, Cm^r, fluorescent marker eGFP: complementation of ΔBCAL3494		46
pSCrhaB2	Broad-range translational fusion vector, Tp^r, rhaR, rhaS-P_{rhaB}, ori_{pBBr1}: complementation of ΔBCAM0992		47
pGPI + BCAL3494 upstream sequence	pGPI-SceI-XCm with ligated upstream sequence BCAL3494, used during deletion	$pGPI_{UL}$	this study
pGPI + BCAL3494 upstream and downstream sequence	pGPI-SceI-XCm with ligated upstream and downstream sequence BCAL3494, used during deletion	$pGPI_{UL-DL}$	this study
pGPI + BCAM0992 upstream sequence	pGPI-SceI-XCm with ligated upstream sequence BCAM0992, used during deletion	$pGPI_{UM}$	this study
pGPI + BCAM0992 upstream and downstream sequence	pGPI-SceI-XCm with ligated upstream and downstream sequence BCAM0992, used during deletion	$pGPI_{UM-DM}$	this study

pJH2 + BCAL3494 sequence	Fusion vector with ligated BCAL3494 sequence, used for complementation	$pJH2_{L3494}$	this study
pSCrhaB2 + BCAM0992 sequence	Fusion vector with ligated BCAM0992 sequence, used for complementation	$pSCrhaB2_{M0992}$	this study

592

593

Supplementary data

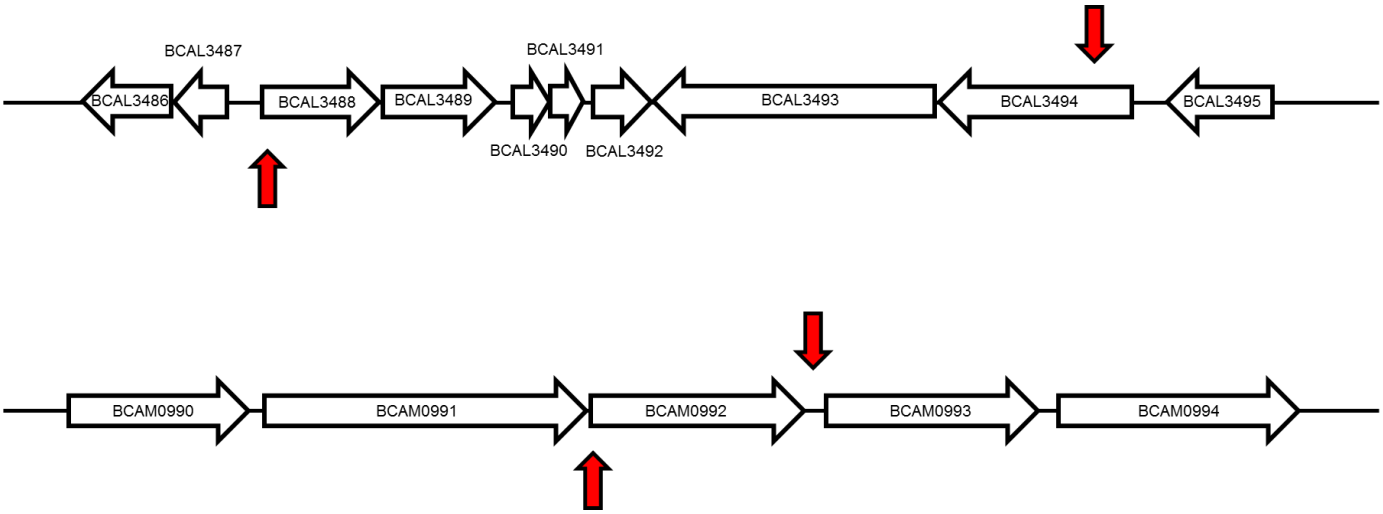

FIGURE S1 Genome context of deleted DNA MTase genes BCAL3494 (top) and BCAM0992 (bottom). The red arrows indicate the boundaries of the deleted part. For gene BCAL3494, adjacent restriction gene BCAL3493, and hypothetical genes BCAL3488 to BCAL3492 were deleted as well.

601

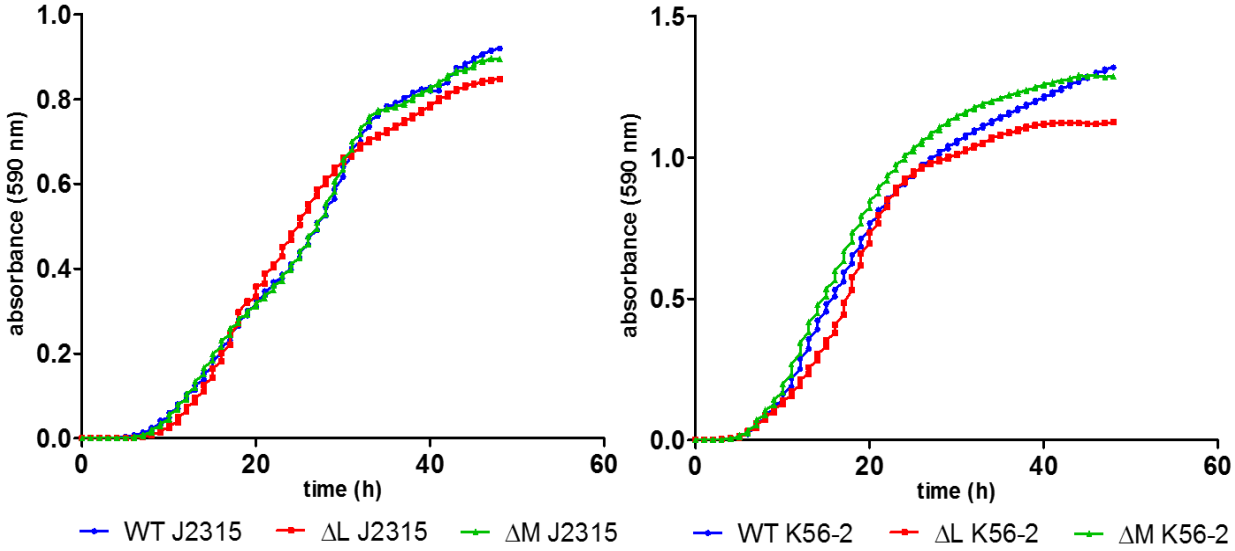

602

603 **FIGURE S2** Growth of *B. cenocepacia* J2315 (left) and K56-2 (right) in phosphate
604 buffered minimal medium. (WT: wild type, ΔL: deletion mutant ΔBCAL3494, ΔM:
605 deletion mutant ΔBCAM0992)

606

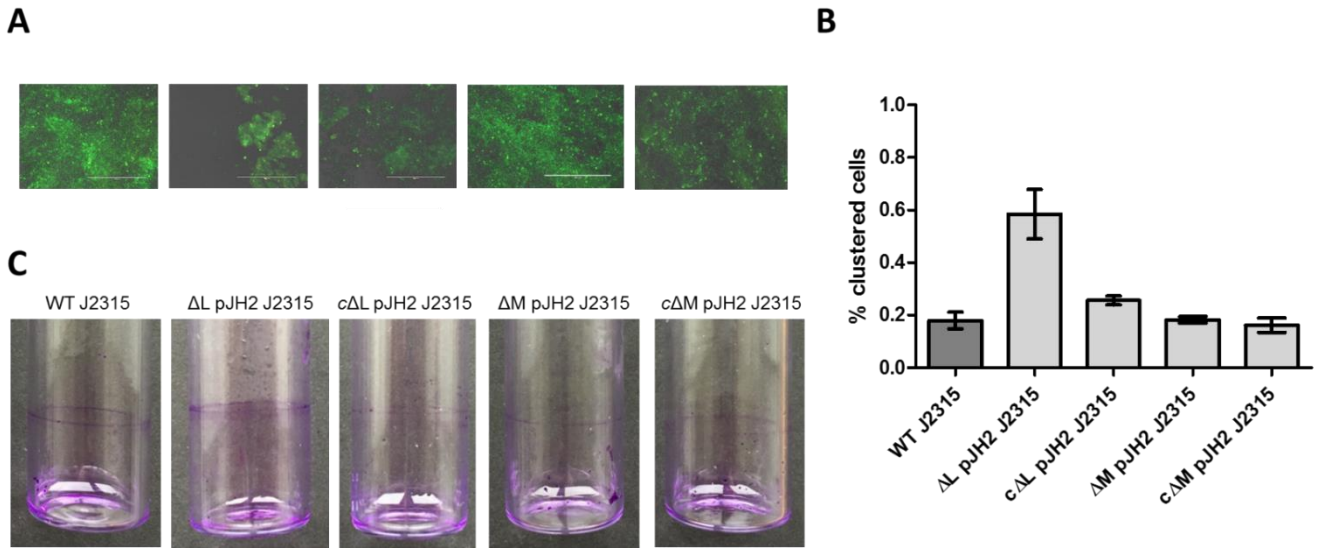

607

608 **FIGURE S3** Biofilm formation, cell aggregation, and pellicle formation of complemented
609 DNA MTase mutants in *B. cenocepacia* J2315. (A) Microscopic images of LIVE/DEAD
610 stained biofilms, grown in microtiter plate wells for 24 h. White bar (200 µm) for scale.
611 (B) Clustering of cells in planktonic cultures, analyzed with flow cytometry. (C) Pellicle
612 formation inside glass tubes after 24 h of static incubation, stained with crystal violet.
613 (n=3, error bars represent the Standard Error of the Mean (SEM). WT: wild type, ΔL
614 pJH2 and ΔM pJH2: mutant strains with empty vector pJH2 (vector control), *c*ΔL pJH2
615 and *c*ΔM pJH2: deletion mutants complemented with genes BCAL3494 and
616 BCAM0992)

617

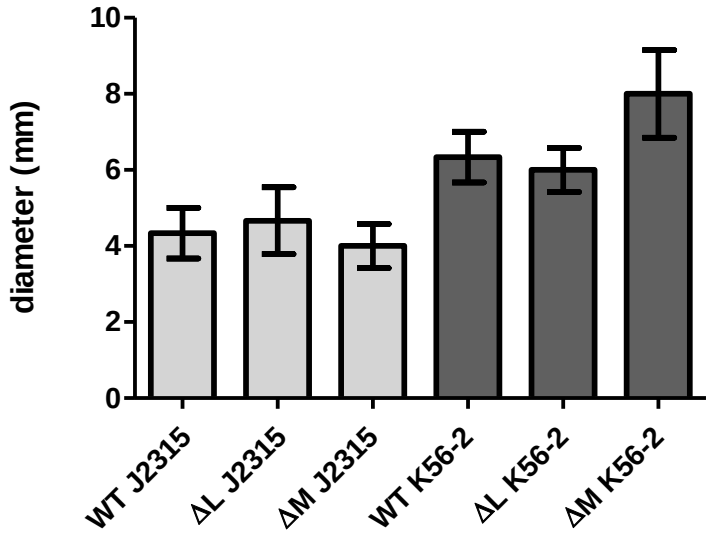

618

619 **FIGURE S4** Swarming motility of DNA MTase deletion mutants. Diameters were
620 measured after 24 h. (n=3, error bars represent the SEM. WT: wild type, ΔL: deletion
621 mutant ΔBCAL3494, ΔM: deletion mutant ΔBCAM0992)

622

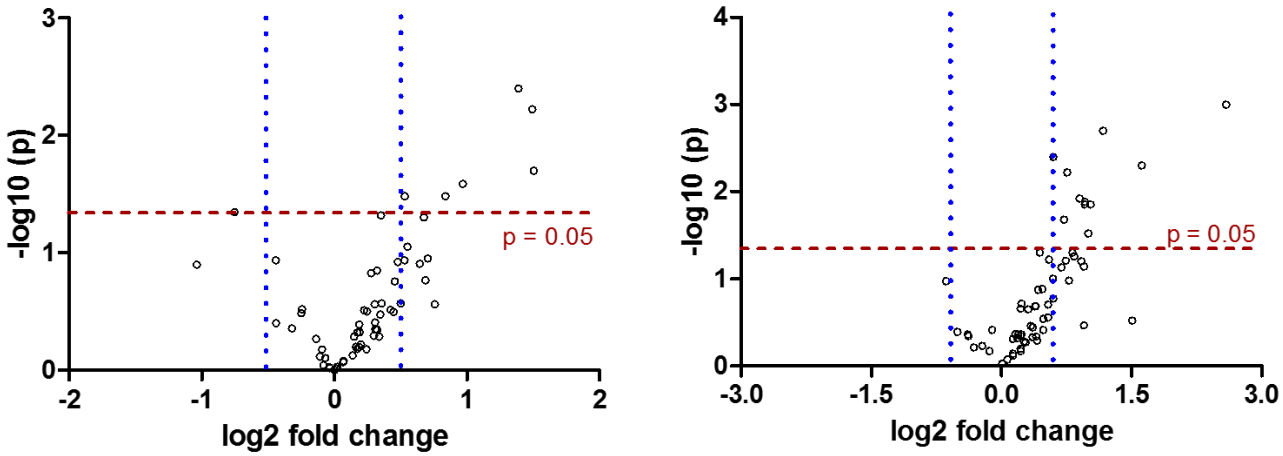

623

624 **FIGURE S5** Differential expression (Volcano plots) of all genes with methylated
625 promoter region in J2315 (left) and K56-2 (right) for which expression was quantified
626 using qPCR. Cut-offs were drawn at fold changes -1.5 and 1.5 (blue) and at p-value
627 0.05 (red). All genes outside of these cut-offs were considered significantly up- or
628 downregulated.

629

630

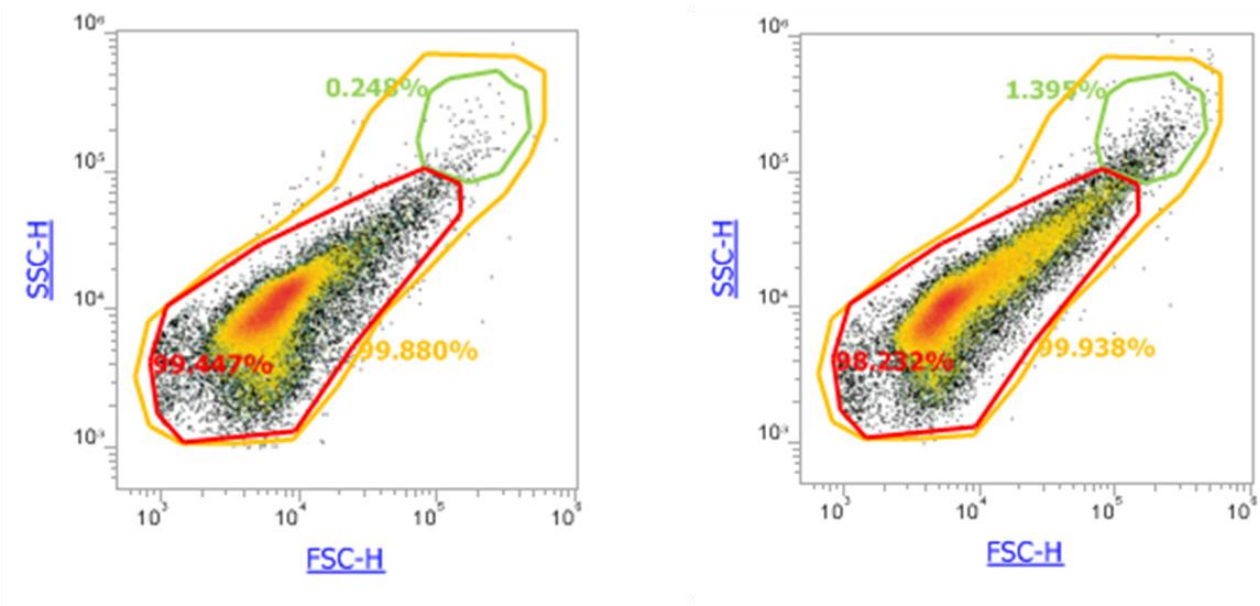

631

632 **FIGURE S6** Quantification of the number of clusters in wild type J2315 (left) and
633 ΔBCAL3494 J2315 (right) (SSC: side scatter, FSC: forward scatter, green circle
634 indicates clusters, red circle indicates main population (ranging from approx. 10^3 to 10^5
635 for both FSC and SSC)).

636

637 **TABLE S1** All DNA MTase genes in the *B. cenocepacia* J2315 genome identified by
638 REBASE (* BLASTn search against the genus *Burkholderia*, default screening
639 parameters were used).

Locus Tag	Name	Location	Predicted type MTase (48)	Widely distributed in genus *Burkholderia* *
BCAL3494	M.BceJI	CHR 1	Type III	✓
BCAM1036	M.BceJII	CHR 2		
pBCA072	M.BceJIII	PLASMID		
BCAM0992	M.BceJIV	CHR 2		✓
BCAL0178	M.BceJ178P	CHR 1	Type II	
BCAL0414	M.BceJ414P	CHR 1	Type I	

640

641 **TABLE S2** Methylation motifs in *B. cenocepacia* (methylated bases in bold and
642 underlined, 6mA: N_6-methyl adenine, 4mC: N_4-methyl cytosine, F: forward strand, R:
643 reverse strand). * wild type strain J2315 percentages.

Motif	Methylation	Strand	Called modified motifs * (%)	Methylation of motif by
CAC**A**G	6mA	F	6834/6836 (99.9)	BCAL3494
G**T**WW**A**C	6mA	F+R	961/982 (97.8)	BCAM0992
GCG**GC**CGC	4mC	F+R	1738/6850 (25.3)	unknown

644

645 **TABLE S3** Genes with methylated promoter region (CACAG motif) in J2315
646 (methylated promoter regions in K56-2 are indicated with '+', non-methylated promoter
647 regions with '-').

	Locus tag	Gene function	Methylated in K56-2
		Intermediary metabolism	
1	BCAL0627	putative hydrolase	+
2	BCAL1059	ArgD bifunctional N-succinyldiaminopimelate-aminotransferase/acetylornithine transaminase protein	+
3	BCAL1086	putative lipoprotein	+
4	BCAL1249	putative PHB depolymerase	+
5	BCAL1515	SucA 2-oxoglutarate dehydrogenase E1 component	+
6	BCAL1762	acetyltransferase (GNAT) family protein	+
7	BCAL1796	putative saccharopine dehydrogenase	+
8	BCAL1924	MoeA3 molybdopterin biosynthesis protein	+
9	BCAL2767	ArgF ornithine carbamoyltransferase	+
10	BCAL2782	PdxH pyridoxamine 5'-phosphate oxidase	+
11	BCAL2796	benzoylformate decarboxylase	+
12	BCAM0941	*gnd* 6-phosphogluconate dehydrogenase	+

13	BCAM1128	putative glycosyl transferase family protein	+
14	BCAM1204	DadX alanine racemase	+
15	BCAM1262	IlvD dihydroxy-acid dehydratase	+
16	BCAM1353	*ald* alanine dehydrogenase	+
17	BCAM1459	AtoE short-chain fatty acid transporter	+
18	BCAM1485	ornithine cyclodeaminase	+
19	BCAM2380	putative D-isomer specific 2-hydroxyacid dehydrogenase	+
20	BCAM2738	IspH 4-hydroxy-3-methylbut-2-enyl diphosphate reductase	+
21	BCAS0223	AfcC putative fatty acid desaturase	+
22	BCAS0257	putative acetyltransferase	+
23	BCAS0324	sugar ABC transporter ATP-binding protein	+
		Regulation	
1	BCAL0003	MarR family regulatory protein	+
2	BCAL0003	MarR family regulatory protein	+
3	BCAL1457	LysR family regulatory protein	+
4	BCAL1477	LysR family regulatory protein	+
5	BCAL2443	GntR family regulatory protein	+
6	BCAL2465	TetR family regulatory protein	+
7	BCAL2465	TetR family regulatory protein	+
8	BCAL3190	IclR family regulatory protein	+
9	BCAM0466	LysR family regulatory protein	+
10	BCAM0466	LysR family regulatory protein	+
11	BCAM0618	two-component regulatory system response regulator protein	+
12	BCAM0820	hybrid two-component system kinase-response regulator protein	+
13	BCAM0886	LysR family regulatory protein	+
14	BCAM1415	AraC family regulatory protein	+
15	BCAM1755	GntR family regulatory protein	+
16	BCAM1975	AraC family regulatory protein	+
17	BCAS0235	two-component regulatory system, response regulator protein	+
		Membrane and transport	
1	BCAL2005	putative membrane protein	+
2	BCAL2648	putative outer membrane protein	+
3	BCAL2648	putative outer membrane protein	+
4	BCAL2677	putative permease protein	+
5	BCAL2948	putative membrane protein	+
6	BCAL3490	putative exported protein	+
7	BCAM0837	putative membrane protein	+
8	BCAM0837	putative membrane protein	+
9	BCAM0945	putative membrane protein	+
10	BCAM1797	putative ion channel protein	+
11	BCAM2683	putative cation-transporting ATPase membrane protein	+

		Protein synthesis	
1	BCAL0024	GidA tRNA uridine 5-carboxymethylaminomethyl modification enzyme	+
2	BCAL0115	RpsU 30S ribosomal protein S21	+
3	BCAL0115	RpsU 30S ribosomal protein S21	+
4	BCAL0423a	RpmH 50S ribosomal protein L34	+
5	BCAL0990	RpmF 50S ribosomal protein L32	+
6	BCAL1553	putative ribonuclease	+
7	BCAL2880	RpmF 50S ribosomal protein L32	+
8	BCAL3303	queA S-adenosylmethionine:tRNA ribosyltransferase-isomerase	+
9	BCAL3530	HupA DNA-binding protein HU-alpha	+
10	BCAM0131	HchA chaperone protein	+
11	BCAM0158	putative diguanylate phosphodiesterase	+
		Electron transport and ATP synthesis	
1	BCAL0194	putative oxidoreductase	+
2	BCAL0389	DsbC thiol:disulfide interchange protein	+
3	BCAL0626	putative 2-nitropropane dioxygenase	+
4	BCAL3276	PpnK NAD(+)/NADH kinase family protein	+
5	BCAL3475	putative molybdopterin-containing oxidoreductase	+
		Chromosome replication	
1	BCAL0423	DnaA chromosomal replication initiation protein	+
2	BCAL0423	DnaA chromosomal replication initiation protein	+
		Proteins involved in DNA methylation	
1	BCAL0509	MetK S-adenosylmethionine synthetase	+
		Hypothetical proteins and pseudogenes	
1	BCAL0362	conserved hypothetical protein	+
2	BCAL0610	conserved hypothetical protein	+
3	BCAL0761	conserved hypothetical protein	+
4	BCAL0763	conserved exported protein	+
5	BCAL0768	conserved hypothetical protein	+
6	BCAL0794	conserved hypothetical protein	+
7	BCAL0810	pseudogene	+
8	BCAL3259	pseudogene	+
9	BCAL3259	pseudogene	-
10	BCAL3483	hypothetical protein	+
11	BCAM0295	conserved hypothetical protein	+
12	BCAM0397	conserved hypothetical protein	+
13	BCAM0488	conserved hypothetical protein	+
14	BCAM0888	conserved hypothetical protein	+
15	BCAM2073	hypothetical protein	+
16	BCAM2254	hypothetical protein	+
17	BCAM2287	hypothetical protein	+

18	BCAM2417	conserved hypothetical protein	+
19	BCAM2609	hypothetical protein	+
20	BCAM2635	hypothetical protein	+
21	BCAS0773	hypothetical protein	+

TABLE S4 Genes with methylated promoter region (GTWWAC motif) in J2315 (methylated promoter regions in K56-2 are indicated with '+', non-methylated promoter regions with '-').

	Locus tag	Gene function	Methylated in K56-2
		Intermediary metabolism	
1	BCAL0064	AcoD acetaldehyde dehydrogenase	+
2	BCAL0162	GmhA phosphoheptose isomerase	+
3	BCAL0508	LpxL lipid A biosynthesis myristoyl acyltransferase	+
4	BCAL0709	LipB lipoate-protein ligase B	+
5	BCAL0995	AcpP acyl carrier protein	+
6	BCAL1290	undecaprenyl pyrophosphate phosphatase	+
7	BCAL1467	AroC chorismate synthase	+
8	BCAL1478	putative hydrolase	+
9	BCAL1556	RpiA ribose-5-phosphate isomerase A	+
10	BCAL1938	family C40 cysteine peptidase	+
11	BCAL2406	WabR putative glycosyltransferase	+
12	BCAL2419	glycosyl hydrolases family protein	+
13	BCAL2701	ArgD acetylornithine transaminase protein	+
14	BCAL2875	AcpP acyl carrier protein	+
15	BCAL2942	CysM cysteine synthase B	+
16	BCAL3153	putative lipoprotein	+
17	BCAL3179	LdhA putative D-lactate dehydrogenase	+
18	BCAM0013	putative acetyltransferase	+
19	BCAM1679	putative lysylphosphatidylglycerol synthetase	+
20	BCAM1761	putative lipoprotein	+
21	BCAM2511	GarD putative D-galactarate dehydratase	+
22	BCAM2737	putative glycosyl transferase	+
23	BCAS0065	putative glutathione S-transferase	+
		Membrane and transport	
1	BCAL0121	AqpZ aquaporin Z	+
2	BCAL0126	MotA chemotaxis protein	+
3	BCAL0824	putative membrane protein	+
4	BCAL1525	*flp* type pilus subunit	+
5	BCAL1808	putative membrane protein	+
6	BCAL2301	putative exported protein	+

7	BCAL2370	putative membrane protein	+
8	BCAM0837	putative membrane protein	+
9	BCAM0885	putative membrane protein	+
10	BCAM0988	putative exported protein	+
11	BCAM1669	putative exported protein	+
12	BCAM1726	putative exported protein	+
13	BCAM1743	periplasmic solute-binding protein	+
14	BCAM1830	putative exported protein	+
15	BCAM2555	putative exported protein	+
16	BCAM2827	putative exported protein	+
17	BCAM2828	putative membrane protein	+
		Regulation	
1	BCAL0054	MerR family regulatory protein	+
2	BCAL0444	GntR family regulatory protein	+
3	BCAL0497	two-component regulatory system, sensor kinase protein	+
4	BCAL2606	two-component regulatory system, response regulator protein	+
5	BCAM0076	TetR family regulatory protein	+
6	BCAM0085	TetR family regulatory protein	+
7	BCAM0483	ADA-like AraC family regulatory protein	+
8	BCAM2589	IclR family regulatory protein	+
9	BCAS0007	TetR family regulatory protein	+
10	BCAS0258	GntR family regulatory protein	+
		Electron transport and ATP synthesis	
1	BCAL0080	putative cytochrome	+
2	BCAL2145	NADH-ubiquinone oxidoreductase subunit	+
3	BCAL2415	PurT phosphoribosylglycinamide formyltransferase 2	+
4	BCAL3187	putative oxidoreductase	+
5	BCAL3362	putative oxidoreductase	+
6	BCAL3432	cytochrome c assembly protein	+
		DNA transposition	
1	BCAL2216	putative transposase	+
2	BCAL3238	putative transposase	+
3	BCAL3295	putative transposase	+
		Protein synthesis	
1	BCAL1856	RimO ribosomal protein S12 methylthiotransferase	+
2	BCALr3484	tRNA-Val	+
		Chromosome replication	
1	BCAL0079	*rep* ATP-dependent DNA helicase	+
		Proteins involved in DNA methylation	
1	BCAL0747	putative methyltransferase	+
		Other proteins	

1	BCAL0825	UvrA excinuclease ABC subunit A	+
2	BCAL0849	subfamily M48B metalopeptidase	+
3	BCAL2643	SodC superoxide dismutase	+
4	BCAL2749	putative diguanylate phosphodiesterase	+
5	BCAL2940	putative histone deacetylase-family protein	+
6	BCAM1362	putative penicillin-binding protein	+
7	BCAS0010	putative activator of osmoprotectant transporter	+
8	BCAS0293	AidA nematocidal protein	+
		Hypothetical proteins and pseudogenes	
1	BCAL0362	conserved hypothetical protein	+
2	BCAL0434	putative exported protein	+
3	BCAL1442	conserved hypothetical protein	+
4	BCAL2175	conserved hypothetical protein	+
5	BCAL3193	conserved hypothetical protein	+
6	BCAM0008	conserved hypothetical protein	+
7	BCAM1874-2	pseudo	+
8	BCAM2207	conserved hypothetical protein	+
9	BCAM2289	conserved hypothetical protein	+

TABLE S5 List of TFs that bind to methylation motifs CACAG and GTWWAC, predicted by Virtual Footprint. Bold sequences represent methylation motifs. (Consensus sequence based on TF binding in *E. coli* K12)

Transcription Factor	Strand	Score	Consensus sequence
CACAG motif			
GlpR	-	6.07	**TGTG**TTCTAATTTCATTTAG
GTWWAC motif			
ArcA	+	7.39	T**GTTAAC**ATG
ArcA	-	7.22	T**GTTAAC**ACG
OxyR	-	4.49	CAT**GTTAAC**AC
OxyR	+	4.11	CGT**GTTAAC**AT
Fis	-	3.49	GACGCGCAT**GTTAAC**
Fur	-	2.55	AT**GTTAAC**

TABLE S6 Overview of all primers used for construction and complementation of gene deletion mutants.

Primers	Sequence (5' 3')	Abbreviation
	ΔBCAL3494 primers	
Flanking sequences		
upstream sequence F	ATATGAATTCCCAACGGTTTCAAGGAGACG	UL3494-EcoRI

upstream sequence R	ATATAGATCTGGCGGATCGATGTAGACGAG	UL3494-Bgl II
downstream sequence F	ATATAGATCTGGGATGCAAGAAGGCTCATC	DL3494-Bgl II
downstream sequence R	TTTACCCGGGATAGGTCTCGCGCTGGTGTC	DL3494-SmaI
Control primers		
Overlapping sequence insert control F	ATGGAGAATCCCGGAAGAAG	joinL3494-F
Overlapping sequence insert control R	TGCTGTTTCATCTGGTGCTC	joinL3494-R
BCAL3494 gene control F	GGCAGCGATTTCGTCTATCC	geneL3494-F
BCAL3494 gene control R	CACTTCGTGCTCGTCGATGT	geneL3494-R
Complementation		
BCAL3494 complementation F	TTTGGATCCTCGTCCTGTTTCAGCCTTTGAGC	L3493-4-ov-BamHI
BCAL3494 complementation R	TTTTCTAGAGCTTTCACGCGAATGACAGGATG	L3493-4-ov-XbaI
ΔBCAM0992 primers		
Flanking sequences		
upstream sequence F	ATATGAATTCGATCTACCTGAAGCGCGAAG	UM0992-EcoRI
upstream sequence R	ATATGCTAGCGGCTCTTCGATCAGGTCACG	UM0992-NheI
downstream sequence F	ATATGCTAGCCGTATGAGACCGGAGCAAGC	DM0992-NheI
downstream sequence R	ATATAGATCTCACTTGACCCACAGGCCTTC	DM0992-Bgl II
Control primers		
Overlapping sequence insert control F	ATACCTCGGTGCAGCTGATC	joinM0992-F
Overlapping sequence insert control R	CAATGCTCGAAACATCCAGA	joinM0992-R
BCAM0992 gene control F	AACGATTCGGACAAGCGTTC	geneM0992-F
BCAM0992 gene control R	CGGTCCCAGATGATCTCGTT	geneM0992-R
Complementation		
BCAM0992 complementation F	AATAATAATCATATGCGTGACCTGATCGAAGAG	M0992-ov-NdeI
BCAM0992 complementation R	TTTGGATCCCATACGATGTATGCGTTGCGTTC	M0992-ov-BamHI
pGPI-SceI-XCm MCS primers		
MCS plasmid sequence insert control F	AACAAGCCAGGGATGTAACG	MCS-B-F
MCS plasmid sequence insert control R	TGTTCGGCCAGATAGAAACC	MCS-B-R

659

660 **TABLE S7** Primers used in qPCR experiments.

Primers	Sequence (5' 3')	Primers	Sequence (5' 3')
M0918-F	GAGATGAGCACCGATCACAC	**L0024-F**	TACAGGCGTGATCGAAGGTG
M0918-R	CCTTCGAGGAACGACTTCAG	**L0024-R**	GGAAGATCTGGTGCGATTCC
L0003-F	AATGGCCTGAATTCCTGACG	**L0509-F**	GGTGATGGTCAACACGTTCG
L0003-R	GTGATGCACGGTCTTCTTCG	**L0509-R**	CCGTAAGCTGCCGTCTTCTC
L0423-F	AGCTGGACTGGGTCAAGAGC	**L2465-F**	GGCTGTCTGATCGTGCTGTC
L0423-R	GGATCGAGGACGAACTGGAC	**L2465-R**	ATGCCCTGTTGAACCGTCAC
M0820-F	ACGTCTACCGGACCGAACAC	**L2767-F**	AGACCTATCACCCGCTGCAC
M0820-R	TCGAGCACGATTTCGTTGAG	**L2767-R**	ACGGGTGGTATTCGTTCGTC

L1059-F	GATGCTGACGACGAACGAAC	**L2782-F**	AGCCGAACACGATGACACTC
L1059-R	GTCCTTGAAGATGCCGAAGC	**L2782-R**	CTTGCGGCTTTCGTAATTGG
L1457-F	CAGCAGATGAATTCGACCAC	**L3303-F**	GACGAGACGCGCTACCAGAC
L1457-R	TCGACGTAAGCGAGGATCTG	**L3303-R**	GGTCGTACCACTCGCTGTGC
S0223-F	ATGCTCGTGTCGTTTCATGC	**L0054-F**	AGCGCACCGATTCGAACTAC
S0223-R	ACTGGTCGCCGTAGTCGAAG	**L0054-R**	ACGTGTCCGATGTGATCGTC
M2738-F	GCTGAGCGAACAGGTTGACG	**L0162-F**	GCATCCACGAAGTCCATCTG
M2738-R	ACCATTCGGCCTTCACTTCC	**L0162-R**	AATCCTCACCCAGCAGCATC
M1262-F	ACCGCGAACTCGATGAACTG	**L1556-F**	ACTGCTTCATCGACGCACTC
M1262-R	GGTGCAGGATCGTGTTGGTC	**L1556-R**	CGTTCAGGTCGAACACCTTG
L0079-F	GTCAACCAGCTCACCGTCTG	**L2415-F**	GTGAAGCCCGTGATGTCGTC
L0079-R	CTTCCACAGCGAGATGATGC	**L2415-R**	GACCGGCTCGCAGAAGTAGG
L0126-F	TGATGGCGCTTCTTTACGTG	**S0258-F**	AAGATGCGGGAACTGATCGAC
L0126-R	ATTCGACGATGTGGTGATCG	**S0258-R**	ATGAAACACCCAGCCGATACG
L0508-F	TCGTCTGAGGGTGTTCAAGC	**M0941-F**	ACAAGCAATCGGTGTGATCG
L0508-R	ATCAGCGGAATCTGCTCCTC	**M0941-R**	AGCGTATAGGTCGGCACCAG
L0709-F	GCGGCGTATAATCTCGCTTC	**M1415-F**	AGACGACAACGCGAAACTCG
L0709-R	ATGTCGACGGTTTCCAGTCC	**M1415-R**	ATCAGGTACGACGGCGACAG
L2701-F	TCACGTTCGACCACAGCTTC	**M0076-F**	TGCCGCCTTTGTACTCATGG
L2701-R	GACGCGATGTTGTTCAGCTC	**M0076-R**	GCGACACGGAAATGATCTCG
L2942-F	AAGCCTACATGCCGACCATC	**M1362-F**	GATCGTGGTCGTCGTGTTCC
L2942-R	GATCGCAGACGATGAACACG	**M1362-R**	GTCTTGTCGTTGCCGAGACG
L2406-F	TGCCGAGATTGCTGTTCAAG	**L1515-F**	CGCAAGCAACCTGTACTTCG
L2406-R	AGCAACGGTGTCAGCAACAG	**L1515-R**	GTCAGGCGATTCAGGATGTG

661

662 **TABLE S8** List of primers used for construction of translational eGFP reporter fusion
663 plasmids.

Gene	Primers	Sequence (5' 3')
BCAL0079	F-eGFP-L0079-BamHI	ATATGGATCCTGCGTATTGTGTCCGATCA
	R-eGFP-L0079-EcoRI	ATATGAATTCCATGATGGCGGATGGTGTT
BCAL1515	F-eGFP-L1515-BamHI	ATATGGATCCGGTGCTTTCAGGCACATTTC
	R-eGFP-L1515-EcoRI	ATATGAATTCGCCGAACAGATAGGAGTTCAG
BCAM0820	F-eGFP-M0820-BamHI	ATATGGATCCCTGCCGATTCGGAGTATCTG
	R-eGFP-M0820-EcoRI	ATATGAATTCATCCGAGGCATTATCACTGCT
Plasmid insert	F-pJH2	CGTAGAGGATCTGCTCATGTTTGAC
	R-pJH2	GACGTAAACGGCCACAAGTTCA

664

665 ## References

666 1. Mahenthiralingam E, Urban TA, Goldberg JB. 2005. The multifarious,
667 multireplicon *Burkholderia cepacia* complex. Nat Rev Microbiol 3:144–56.
668 2. Coenye T. 2010. Social interactions in the *Burkholderia cepacia* complex: biofilm
669 formation and quorum sensing. Future Microbiol 5:1087–99.
670 3. Mahenthiralingam E, Vandamme P. 2005. Taxonomy and pathogenesis of the
671 *Burkholderia cepacia* complex. Chron Respir Dis 2:209–17.
672 4. Lipuma JJ. 2010. The Changing Microbial Epidemiology in Cystic Fibrosis. Clin
673 Microbiol Rev 23:299–323.
674 5. Sousa SA, Feliciano JR, Pita T, Guerreiro SI, Leitão JH. 2017. *Burkholderia*
675 *cepacia* Complex Regulation of Virulence Gene Expression : A Review. Genes
676 19:8(1).
677 6. Drevinek P, Mahenthiralingam E. 2010. *Burkholderia cenocepacia* in cystic
678 fibrosis : epidemiology and molecular mechanisms of virulence. Clin Microbiol
679 Infect 16(7):821–30.
680 7. Coutinho CP. 2011. Long-term colonization of the cystic fibrosis lung by
681 *Burkholderia cepacia* complex bacteria: epidemiology, clonal variation, and
682 genome-wide expression alterations. Front Cell Infect Microbiol 1(12):1–11.
683 8. Courtney JM, Dunbar KEA, Mcdowell A, Moore JE, Warke TJ. 2004. Clinical
684 outcome of *Burkholderia cepacia* complex infection in cystic fibrosis adults. J Cyst
685 Fibros 3:93–8.
686 9. Hindo H, Sigley C, Karlson K. 2008. Case Report Cepacia Syndrome in an

687 Adolescent With Cystic Fibrosis. Infectious Diseases in Clinical Practice
688 16(3):198–200.
689 10. Holden MTG, Seth-smith HMB, Crossman LC, Sebaihia M, Bentley SD, Cerden
690 AM, et al. 2009. The Genome of *Burkholderia cenocepacia* J2315 , an Epidemic
691 Pathogen of Cystic Fibrosis Patients. J Bacteriol 191(1):261–77.
692 11. Coenye T, LiPuma JJ. 2003. Population structure analysis of *Burkholderia*
693 *cepacia* genomovar III: Varying degrees of genetic recombination characterize
694 major clonal complexes. Microbiology 149(1):77–88.
695 12. Vandamme P, Holmes B, Coenye T, Goris J, Mahenthiralingam E, LiPuma JJ,
696 Govan JR. 2003. *Burkholderia cenocepacia* sp. nov. - A new twist to an old story.
697 Res Microbiol 154(2):91–6.
698 13. Weinhold B. 2006. Epigenetics: the science of change. Environ Heal Perspect
699 114(3):160–7.
700 14. Sánchez-Romero MA, Cota I, Casadesús J. 2015. DNA methylation in bacteria :
701 from the methyl group to the methylome. Curr Opin Microbiol 25:9–16.
702 15. Sánchez-Romero MA, Casadesús J. 2020. The bacterial epigenome. Nat Rev
703 Microbiol 18(1):7-20.
704 16. Blow MJ, Clark TA, Daum CG, Deutschbauer AM, Fomenkov A, Fries R, et al.
705 2016. The Epigenomic Landscape of Prokaryotes. PLoS Genet 12(2):1–28.
706 17. Casadesús J, Low D. 2006. Epigenetic Gene Regulation in the Bacterial World.
707 Microbiol Mol Biol Rev 70(3):830–56.
708 18. Lacey L. Westphal, Peter Sauvey, Matthew M. Champion, Ian M. Ehrenreich,
709 Steven E. Finkel. 2016. Genomewide Dam Methylation in Stationary Phase.

mSystems 1(6):1–13.

19. Attwood JT, Yung RL, Richardson BC. 2002. DNA methylation and the regulation of gene transcription. Cell Mol Life Sci 59:241–57.

20. Low DA, Casadesús J. 2008. Clocks and switches: bacterial gene regulation by DNA adenine methylation. Curr Opin Microbiol 11(2):106–12.

21. Adhikari S, Curtis PD. 2016. DNA methyltransferases and epigenetic regulation in bacteria. FEMS Microbiol Rev 40(5):575-91.

22. Wion D, Casadesús J. 2006. N6-methyl-adenine: an epigenetic signal for DNA–protein interactions. Nat Rev Microbiol 4(3):183–92.

23. Militello KT, Mandarano AH, Varechtchouk O, Simon RD. 2014. Cytosine DNA methylation influences drug resistance in *Escherichia coli* through increased sugE expression. FEMS Microbiol Lett 350:100–6.

24. Hermann A, Jeltsch A. 2003. Methylation Sensitivity of Restriction Enzymes Interacting with GATC Sites. Biotechniques 34(5):30–3.

25. Flusberg BA, Webster D, Lee J, Travers K, Olivares E, Clark A, et al. 2010. Direct detection of DNA methylation during single-molecule, real- time sequencing. Nat Methods 7(6):461–5.

26. Fang G, Munera D, Friedman DI, Mandlik A, Chao MC, Banerjee O, et al. 2012. Genome-wide mapping of methylated adenine residues in pathogenic *Escherichia coli* using single-molecule real-time sequencing. Nat Biotechnol 30(12):1232–9.

27. Eid J. et al. 2009. Real-time DNA sequencing from single polymerase molecules. Science 323:133–138.

28. Murphy J, Mahony J, Ainsworth S, Nauta A, Sinderen V. 2013. Bacteriophage

Orphan DNA Methyltransferases : Insights from Their Bacterial Origin , Function , and Occurrence. Appl Environ Microbiol 79(24):7547–55.

29. Yadav MK, Park S, Chae S, Song J. 2014. Sinefungin, a Natural Nucleoside Analogue of S-Adenosylmethionine, Inhibits *Streptococcus pneumoniae* Biofilm Growth. Biomed Res Int 2014:156987.

30. Du W, Dubarry N, Passot FM, Kamgoué A, Murray H. 2016. Orderly Replication and Segregation of the Four Replicons of *Burkholderia cenocepacia*. PLoS Genet 12(7):1–27.

31. Roberts RJ, Vincze T, Posfai J, Macelis D. 2005. REBASE — restriction enzymes and DNA methyltransferases. Nucleic Acids Res 33:230–2.

32. McCammon MT, Parks LW. 1981. Inhibition of Sterol Transmethylation by S-adenosylhomocysteine analogs. J Bacteriol 145(1):106–12.

33. Aya R, Sarnacki SH, Llana MN, Gabriela A, Guerra L, Giacomodonato MN, et al. 2015. Dam methylation is required for efficient biofilm production in *Salmonella enterica* serovar Enteritidis. Int J Food Microbiol 193:15–22.

34. Ouellette M, Gogarten JP. 2018. Characterizing the DNA Methyltransferases of *Haloferax volcanii* via Bioinformatics, Gene Deletion, and SMRT Sequencing. Genes 9(3).

35. Casselli T, Tourand Y, Scheidegger A, Arnold WK, Proulx A, Stevenson B, et al. 2018. DNA methylation by restriction modification systems affects the global transcriptome profile in *Borrelia burgdorferi*. J Bacteriol 200(24):1–17.

36. Nandi T, Holden MTG, Didelot X, Mehershahi K, Boddey JA, Beacham I, et al. 2015. *Burkholderia pseudomallei* sequencing identifies genomic clades with

distinct recombination, accessory, and epigenetic profiles. Genome Res 25(1):129–41.

37. Erill I, Puigvert M, Legrand L, Guarischi-Sousa R, Vandecasteele C, Setubal JC, et al. 2017. Comparative analysis of *Ralstonia solanacearum* methylomes. Front Plant Sci 13;8:504.

38. Suzuki MM, Bird A. 2008. DNA methylation landscapes: provocative insights from epigenomics. Nat Rev Genetics 9(6):465–76.

39. Tate PH, Bird P. 1993. Effects of DNA methylation on proteins and gene expression. Curr Opin Genet Dev. 3(2):226-31.

40. Zachary F. Burton. 2018. Evolution Since Coding: Cradles, Halos, Barrels, and Wings. General Transcription Factors and Promoters 27:115–22.

41. Hickman JW, Tifrea DF, Harwood CS. 2005. A chemosensory system that regulates biofilm formation through modulation of cyclic diguanylate levels. Proc Natl Acad Sci USA 102(40).

42. Cooper VS, Staples RK, Traverse CC, Ellis CN. 2014. Parallel evolution of small colony variants in *Burkholderia cenocepacia* biofilms. Genomics 104(6, Part A):447-52.

43. Traverse CC, Mayo-Smith LM, Poltak SR, Cooper VS. 2013. Tangled bank of experimentally evolved *Burkholderia* biofilms reflects selection during chronic infections. Proceedings of the National Academy of Sciences 110(3):E250–E9.

44. Girgis HS, Liu Y, Ryu WS, Tavazoie S. 2007. A Comprehensive Genetic Characterization of Bacterial Motility. PLoS Genet 3(9):1644-60.

45. Balleza E, López-Bojorquez LN, Martínez-Antonio A, Resendis-Antonio O,

Lozada-Chávez I, Balderas-Martínez YI, et al. 2009. Regulation by transcription factors in bacteria: Beyond description. FEMS Microbiol Rev 33(1):133–51.

46. Héberlé É, Bardet AF. 2019. Sensitivity of transcription factors to DNA methylation. Essays Biochem 63(6):727–41.

47. Lenhart JS, Pillon MC, Guarné A, Biteen JS, Simmons LA. 2016. Mismatch repair in Gram-positive bacteria. Res Microbiol 167(1):4–12.

48. Roberts, R. J., Vincze, T., Posfai, J., & Macelis, D. 2015. REBASE-a database for DNA restriction and modification: enzymes, genes and genomes. Nucleic acids research. 43(Database issue), D298–D299.

49. Carver T, Harris SR, Berriman M, Parkhill J, Mcquillan JA. 2012. Artemis : an integrated platform for visualization and analysis of high-throughput sequence-based experimental data. Bioinformatics 28(4):464–9.

50. Altschup SF, Gish W, Pennsylvania T, Park U. 1990. Basic Local Alignment Search Tool. J Mol Biol 215(3):403-10.

51. Hamad MA, Skeldon AM, Valvano MA. 2010. Construction of Aminoglycoside-Sensitive *Burkholderia cenocepacia* Strains for Use in Studies of Intracellular Bacteria with the Gentamicin Protection Assay. Appl Environ Microbiol 76:3170–3176

52. Flannagan RS, Linn T, Valvano MA. 2008. A system for the construction of targeted unmarked gene deletions in the genus *Burkholderia*. Environ Microbiol 10(6):1652–60.

53. Van Acker H, Ostyn L, Sass A, Daled S, Dhaenens M, Deforce D, et al. 2019. The role of small proteins in *Burkholderia cenocepacia* J2315 biofilm formation,

802 persistence and intracellular growth. Biofilm. 2019;1:100001.

803 54. Cardona ST, Valvano MA. 2005. An expression vector containing a rhamnose-
804 inducible promoter provides tightly regulated gene expression in *Burkholderia*
805 *cenocepacia*. Plasmid 54(3):219–28.

806 55. Drago L, Agrappi S, Bortolin M, Toscano M, Romanò CL, Vecchi E De. 2016.
807 How to Study Biofilms after Microbial Colonization of Materials Used in
808 Orthopaedic Implants. Int J Mol Sci.17(3): 293.

809 56. Kong EF, Tsui C, Kucharíková S, Andes D. 2016. Commensal Protection of
810 *Staphylococcus aureus* against Antimicrobials by *Candida albicans* Biofilm Matrix.
811 7(5):1–12.

812 57. Kobayashi K. 2007. *Bacillus subtilis* Pellicle Formation Proceeds through
813 Genetically Defined Morphological Changes. J Bacteriol 189:4920–31.

814 58. Sass AM, Van Acker H, Förstner KU, Van Nieuwerburgh F, Deforce D, Vogel J, et
815 al. 2015. Genome-wide transcription start site profiling in biofilm-grown
816 *Burkholderia cenocepacia* J2315. BMC Genomics 16:775.

817 59. Münch R, Hiller K, Grote A, Scheer M, Klein J, Schobert M, Jahn D. 2005. Virtual
818 Footprint and PRODORIC: An integrative framework for regulon prediction in
819 prokaryotes. Bioinformatics 21(22):4187–9.

820